The contributions of S_1 site residues to substrate specificity and allosteric

behaviour of *Lactococcus lactis* prolidase

A Thesis Submitted to the College of

Graduate Studies and Research

In Partial Fulfillment of the Requirements

For the Degree of Master of Science

In the Department of Food & Bioproduct Sciences

University of Saskatchewan

Saskatoon

By

Keke Hu

Permission to Use

In presenting this thesis in partial fulfilment of the requirements for a Postgraduate degree from the University of Saskatchewan, I agree that the Libraries of this University may make it freely available for inspection. I further agree that permission for copying of this thesis in any manner, in whole or in part, for scholarly purposes may be granted by the professor or professors who supervised my thesis work or, in their absence, by the Head of the Department or the Dean of the College in which my thesis work was done. It is understood that any copying or publication or use of this thesis or parts thereof for financial gain shall not be allowed without my written permission. It is also understood that due recognition shall be given to me and to the University of Saskatchewan in any scholarly use which may be made of any material in my thesis.

Requests for permission to copy or to make other use of material in this thesis in whole or part should be addressed to:

Head of the Department of Food and Bioproduct Sciences

University of Saskatchewan

Saskatoon, Saskatchewan (S7N 5A8)

ABSTRACT

Three residues, Phe190, Leu193 and Val302, which have been proposed to define the S_1 site of prolidase of *Lactococcus lactis* NRRL B-1821 (*L. lactis* prolidase), may limit the size and polarity of specific substrates accepted by this enzyme (Yang, S. I., and Tanaka, T. 2008. Characterization of recombinant prolidase from *L. lactis* changes in substrate specificity by metal cations, and allosteric behavior of the peptidase. FEBS J. **275**, 271-280). These residues form a hydrophobic pocket to determine the substrate specificity of *L. lactis* prolidase towards hydrophobic peptides, such as Leu-Pro and Phe-Pro, while little activity was observed for anionic Asp-Pro and Glu-Pro. It is hypothesized that the substrate specificity of *L. lactis* prolidase would be changed if these residues are substituted with hydrophilic amino acid residues individually or in combinations by site-directed mutagenesis (SDM). In addition to the changes in substrate specificity, other characteristics of wild type prolidase, such as allosteric behaviour and substrate inhibition may receive influences by the mutations (Yang & Tanaka, 2008). To test this hypothesis, mutations were conducted on these three residues at the S_1 site. Mutated *L. lactis* prolidases were subsequently analyzed in order to examine the roles of these residues in the substrate specificity, allosteric behaviour, pH dependency, thermal dependency and metal dependency of prolidase. The results showed the significant changes in these kinetic characteristics of single mutants, such as L193E, L193R, V302D and V302K and double mutants, L193E/V302D and L193R/V302D. Leu193 was suggested to be a key residue for substrate binding. The mutants L193R, V302D, L193R/V302D and L193E/V302D lost their allosteric behaviour, and the substrate inhibition of the wild type was no longer observed in V302D and L193E/V302D. The results indicated Val302 to be more important for these properties than other S_1 site residues. Moreover, together with the observations in molecular modelling of the mutants, it was proposed that interactions of Asp302 with Arg293 and His296 caused the loss of

allosteric behaviour and substrate inhibition in the V302D mutant.   The investigations on the pH dependency suggested that His296 acted as proton acceptor in *L. lactis* prolidase's catalysis.   It was expected that the electrostatic microenvironment surrounding His296 was influenced by the charged mutated residues and side chains of dipeptide substrates, thus the protonation of His296 was affected.   It was suggested that the introduced positive charge would stabilize the deprotonated form of His296 thus to maintain the activities of the mutants in more acidic condition compared to wild type prolidase.   The study of thermal dependency revealed that all non-allosteric prolidases had higher optimum temperatures, suggesting that the loss of allosteric behaviour resulted in more rigid structures in these prolidases.

ACKNOWLEDGMENTS

TABLE OF CONTENTS

LIST OF TABLES

LIST OF FIGURES

LIST OF ABBREVIATIONS

Å	Angstrom
ABS	absorbance
ANOVA	analysis of variance
BCAA	branch-chain amino acids
BSA	bovine serum albumin
BU	binding unit
CcpA	carbon catabolite control protein A
CodY	a transcriptional regulator protein
D32A	the mutation of aspartate to alanine
DEAE	diethyl-aminoethyl
dNTP	deoxynucleotide triphosphate
*ds*DNA	double-strand DNA
E2	Sindbis virus glycoprotein
ES	enzyme-substrate complex in enzyme mechanism
F190E	the mutation of phenylalanine to glutamate
F190R	the mutation of phenylalanine to arginine
F190T	the mutation of phenylalanine to threonine
GAPDH	glyceraldehyde-3-phosphate dehydrogenase
GAM	generalized additive models
h	Hill constant
INT	*gem*-diolate structure
IPTG	isopropyl β-D-1-thiogalactopyranoside
$K_{0.5}$	affinity constant at 1/2 V_{max}

K_i	substrate inhibition constant
K_m	Michaelis-Menten constant
K_R	affinity constant at R state
K_T	affinity constant at T state
L193E	the mutation of leucine to glutamate
L193E/V302D	the double mutations of leucine to glutamate and valine to aspartate
L202F	the mutation of leucine to phenylalanine
L193R	the mutation of leucine to arginine
L193R/V302D	the double mutations of leucine to arginine and valine to aspartate
L193T	the mutation of leucine to threonine
L202Y	the mutation of leucine to tyrosine
L. lactis	*Lactococcus lactis*
LAB	lactic acid bacteria
LB	Luria-Bertani broth
Lb. bulgaricus	*Lactobacillus delbrueckii* subsp. *bulgaricus*
Lb. casei	*Lactobacillus delbrueckii* subsp. *casei*
Lb. lactis	*Lactobacillus delbrueckii* subsp. *lactis*
lm	linear models
M12L/L56F	the double mutations of methionine to leucine and leucine to phenylalanine
MEROPS	the peptidase database
N112D	the mutation of asparagine to aspartate
NA	neuraminidase
NeuAcα2-3Gal	*N*–acetylneuraminic acids bound to galactose through an α2,3 linkage

NeuAcα2-6Gal	N–acetylneuraminic acids bound to galactose through an α2,6 linkage
O$_w$	water oxygen
O$_p$	peptide oxygen
p-value	the probability of obtaining a result
PCR	polymerase chain reaction
PEP	phosphoenolpyruvate
pepC	aminopeptidase C coding gene
PepD	dipeptidase D
pepN	aminopeptidase N coding gene
PepP	aminopeptidase P
pepQ	prolidase coding gene
PepQ	prolidase
pK_a	acid dissociation constant
PROD	products formation state
QCM	QuikChange^{TM} Site-directed Mutagenesis
QQ plot	quantile-quantile plot
R state	relaxed state of allosteric enzymes
R293S	the mutation of arginine to serine
RM	reaction mixture
RmGAPDH	rabbit muscle glyceraldehyde-3-phosphate dehydrogenase
S	substrate concentration
S35A	the mutation of serine to alanine
SDS-PAGE	sodium dodecyl sulfate polyacrylamide gel electrophoresis
SFR	structure-function relationship
SDM	site-directed mutagenesis
SU	stimulating unit

T state	tense state of allosteric enzymes
TLN	thermolysin
TLP	thermolysin-like protease
TmGAPDH	*Thermotoga maritime* glyceraldehyde-3-phosphate dehydrogenase
TS	transition state in enzyme mechanism
v	velocity
V_{max}	maximum velocity
V302D	the mutation of valine to aspartate
V302K	the mutation of valine to lysine
V302T	the mutation of valine to threonine
WT	wild type
Xaa	amino acid

1 INTRODUCTION

In fermented foods, the hydrolysis of proteins releases peptides and amino acids, which are taste determinants, and some of them exhibit bitterness that is unpleasant to consume. Generally speaking, hydrophobic amino acids (e.g., phenylalanine, leucine, trptophan, isoleucine, tyrosine, valine and proline) and their peptide forms are bitter, and bitterness is more intense in the peptides than in the amino acids. Among the bitter peptides, proline-containing peptides withstand the hydrolysis by general peptidases. Fermented foods generally contain large amounts of these proline-containing peptides that are untouched by general hydrolysis. Therefore, bitterness of proline-containing peptides can be prominent in fermented foods. It implies that proline-specific peptidases can assist the reduction of bitterness through hydrolysis of the bitter proline-containing peptides. Prolidase (EC 3.4.13.9) is one of the proline-specific peptidases, and the only peptidase that can hydrolyze Xaa-Pro dipeptide, the end products left by the general hydrolysis of proteins in fermentations. To date, prolidase from *Lactococcus lactis* (*L. lactis*) has not been fully understood. In the previous studies in Dr. Tanaka's lab (Yang and Tanaka, 2008; Zhang et al., 2009), *L. lactis* prolidase was clarified to be specific to Xaa-Pro where Xaa is a hydrophobic dipeptide, whereas Xaa-Pro with hydrophilic Xaa could not be the substrate of this enzyme. This project aimed to engineer prolidase to have a broader substrate specificity including substrates with hydrophilic Xaa. With application of the modified prolidase, protein hydrolysis could be more efficient, and the bitterness arisen by proline-containing peptides could be diminished in fermented foods.

2 LITERATURE SURVEY

2.1 The Contributions of Prolidase in Foods

2.1.1 Proline-Containing Peptides Exhibit Bitterness

Bitter taste is normally perceived as an undesirable attribute in fermented products such as cheese. Before fermentation, the raw material contains large protein molecules that rarely exhibit taste because their hydrophobic amino acids are concealed in the interior and have no access to the taste receptor cells.   When proteins are hydrolyzed in fermentation, hydrophobic amino acid residues are exposed to the solvent and interact with the taste receptor cells.   The varieties of interactions of peptides with the taste receptors result in many different tastes. Bitter peptides are generally those containing hydrophobic amino acids, such as phenylalanine, leucine, trptophan, isoleucine, tyrosine, valine and proline.   Ishibashi et al. showed that proline-containing peptides are generally bitter (Ishibashi et al., 1988b).   They further investigated the tastes of proline-containing peptides and proposed how the proline-containing tetrapeptides, tripeptides and dipeptides exhibited various degrees of bitterness.   They proposed that two bitter taste determinant factors could be defined within a bitter peptide molecule. These factors were called 'binding unit' (BU) and 'stimulating unit' (SU).   When a peptide had both BU and SU within the molecule, it would show more bitterness.   In a proline-containing peptide, the proline residue acted as BU while the rest of the peptide acted as SU (Ishibashi et al., 1988a).   As a result, proline- containing peptides exhibit the bitterness.   Since free amino acids cannot have BU and SU within the molecule, bitterness of the amino acids is less intense than that of the peptides.   In fact, proline and some other hydrophobic amino acids even show some sweetness.   This implies that bitterness of fermented foods could be diminished by degrading the bitter peptides into free amino acids.

Milk has a high content of proline, although most proline is found in proteins rather than as

2

free proline. For example, cow milk contains 280 mg of total proline per 100 g dry matter (Casey MG, 1985) among which free proline concentration was only 0.19 mg (Ghadimi & Pecora, 1963).   Whereas the taste of fresh milk is less affected by peptides and amino acids, fermented milk products have distinctive tastes through protein hydrolysates.   Some fermented dairy products exhibit bitter tastes, especially when the fermentation processes are shortened to result in partial hydrolysis of bitter peptides.   This bitterness is partially from the proline-containing peptides, which are released from the milk proteins in the process of fermentation.   If the proline-containing peptides are further degraded to free proline, the bitterness of the fermented dairy products would be reduced.

2.1.2 Degradation of Proline-Containing Peptides

Fermentation of milk usually results in a higher concentration of free proline because of the proteolysis through microbial activity.   Free proline concentration reached 51.7 mg per 100g dry matter of cheese after 60 days ripening (Buffa et al., 2005).   Milk is often fermented by the application of lactic acid bacteria (LAB), which are defined as Gram-positive, non-sporulating, catalase-negative, aero-tolerant, acid-tolerant, nutritionally fastidious, strictly fermentative microorganisms that lack cytochromes and produce lactic acids as the major end-product of carbohydrate metabolisms (Christensen et al., 1999).   LABs lack the ability to synthesize some amino acids, thus require exogenous sources of amino acids.   In dairy fermentation, little free amino acids exist while large proteins are abundant.   In order to get the supply of free amino acid, LABs produce a systematic proteolysis and transport system to utilize exogenous proteins. The proteolysis starts by an extracellular protease that hydrolyzes proteins into oligopeptides, which are then taken up by the cells through peptide transport systems for further degradation into shorter peptides and free amino acids by various intracellular peptidases (Christensen et al., 1999; Kunji et al., 1996).

Proline withstands to most general peptidases because of its unique cyclic structure that is formed by its side chain bonding to both nitrogen and α-carbon.   This cyclic structure constrains the dihedral angle ϕ of rotation, and further introduces a fixed bend into peptide chains.

Moreover, the cyclic structure means the imide bonding rather than the amide bonding. In common peptidases, these properties of proline constrain the hydrolysis of proline-containing peptides. Thus proline-specific peptidases are required for efficient hydrolysis of proline-peptides. There are a number of proline-specific peptidases found in microorganisms, plants, animal and human tissues, such as prolyl oligopeptidase (EC 3.4.21.26), dipeptidyl peptidase IV (EC 3.4.14.5), aminopeptidase P (EC 3.4.11.9), prolidase (EC 3.4.13.9), proline iminopeptidase (EC 3.4.11.5), and prolinase (EC 3.4.13.8) (Cunningham, 1997). Among these peptidases, proline iminopeptidase, aminopeptidase P, prolinase and prolidase are often observed in LAB (Christensen et al., 1999).

Among the proline-specific peptidases of LAB, prolidase is particularly interesting. Prolidase is the only peptidase that hydrolyzes Xaa-Pro, which is one of the two ultimate products (Xaa-Pro and Pro-Xaa) of the proteolysis by general peptidases (Christensen et al., 1999). Pro-Xaa can be hydrolyzed by prolinase and iminopeptidase, while only prolidase can hydrolyze Xaa-Pro. Thus prolidase is expected to be unique among general and proline-specific peptidases. Furthermore, Xaa-Pro is always bitterer than the Pro-Xaa counterpart (Ishibashi et al., 1988a) because of the positioning of hydrophobic amino acid (proline) at C-terminus. Prolidase is then suggested to be more effective than prolinase and iminopeptidase to reduce the bitterness exhibited in the fermented dairy products.

2.1.3 Benefits of Free Proline

Proline is the starting material to make hydroxyproline, a building block of collagen. Collagen is a substrate found in the skin and connective tissues, and helps to heal cartilage and to cushion the joints and vertebrae. Therefore proline is absolutely essential to the development and maintenance of healthy skin and connective tissues, especially at the site of traumatic tissue injury. Free proline supplementation may benefit the treatments of conditions such as osteoarthritis, persistent soft tissue strains, and chronic back pain.

The hydrolysis of proline-peptides increases the amount of free proline in fermented dairy products. In addition, fermented dairy products contain ascorbic acid, which is the intrinsic

content of milk and acts as a cofactor for the hydroxylation of proline and lysine residues in procollagen followed by its processing to collagen (Gross, 2000). Therefore, the intake of fermented dairy product may assist the collagen synthesis via these active components of free proline and ascorbic acid.

2.2 General Information of Prolidase

2.2.1 Characteristics of Prolidase

Prolidase has been detected and purified from porcine kidney (Davis & Smith, 1957), porcine and bovine intestine (Sjostrom et al., 1973; Yoshimoto et al., 1983), human organs (Cosson et al., 1992; Endo et al., 1987; Myara et al., 1994; Ohhashi et al., 1990) and many microorganisms (Morel *et al.*, 1999; Rantanen & Palva, 1997; Stucky *et al.*, 1995).

Studies of prolidases from various LABs revealed that prolidase was a metalloprotease with a calculated pI of 6.0 and a molecular mass of 41 kDa (Morel *et al.*, 1999; Rantanen & Palva, 1997; Stucky *et al.*, 1995). Prolidase from *Lactobacillus delbrueckii* subsp. *Bulgaricus* CNRZ 397 had the optimum activity in the range of 45~50°C, and the optimum pH 6.0 (Morel et al., 1999). This prolidase showed preference to Xaa-Pro dipeptides with hydrophobic amino acid at the N-terminal, and little activity to Gly-Pro and Pro-Pro (Morel *et al.*, 1999; Rantanen & Palva, 1997). Prolidases were completely inhibited by the metalloprotease inhibitors EDTA and 1,10-phenanthroline and activated by varieties of cations like Ca^{2+}, Mg^{2+}, Mn^{2+}, Fe^{3+} and Co^{2+}. Zinc was suggested to be the essential cation to *Lb. bulgaricus* prolidase activity (Morel et al., 1999), while other prolidases required different divalent cations as cofactors, such as Mn^{2+} for *Lb. casei* prolidase (Fernandez-Espla et al., 1997). The studies of SDS-PAGE and non-denaturing size-exclusion chromatography on *Lb. bulgaricus* prolidase suggested that this enzyme was a homodimer (Morel et al., 1999), and the similar studies on *L. lactis* prolidase also revealed that it was a homodimer with a molecular mass of 80 kDa (Yang & Tanaka, 2008).

L. lactis prolidase was cloned and expressed in *E.coli* (Yang & Tanaka, 2008). This prolidase showed its maximum activity between pH 6 and 7 with Zn^{2+} or Mn^{2+} at 50°C. *L. lactis* prolidase preferred hydrophobic Leu-Pro and Phe-Pro in the presence of zinc while Gly-Pro,

Pro-Pro, Asp-Pro, Glu-Pro, Leu-Leu-Pro, and Leu-Val-Pro could not be hydrolyzed. Interestingly Arg-Pro was a better substrate than Leu-Pro when Mn^{2+} was used as the catalytic cation, though the activity was lower than that of Leu-Pro in the presence of Zn^{2+}. Another uniqueness of this prolidase was observed as allosteric behaviour towards Leu-Pro and Arg-Pro substrates.

2.2.2 Impact of Prolidase on Human Health

Prolidase plays an important role in human health. Prolidase deficiency is a rare autosomal recessive disease characterized by chronic ulcerative dermatitis, mental retardation, frequent infections and massive urinary excretion of iminodipeptides (Goodman et al., 1968). It was reported that the enzyme activity to Gly-Pro was almost totally deficient in patients with prolidase deficiency (Arata et al., 1979). The prolidase and prolinase (Pro-Xaa dipeptidase) activities have been determined in erythrocytes from patients with chronic uremia and in plasma from patients with alcoholic liver disease, and found to be enhanced significantly in these diseases (Brosset et al., 1988; Gejyo et al., 1983). Latest research reported that some sulfur amino acids such as stereoiosomer and D,L-Methionine could enhance the prolidase activity. And the ointment containing glycine and D,L-Methionine with $MnCl_2$ was found to be clinically useful for the treatment of leg ulcers of patients with prolidase deficiency (Uramatsu et al., 2007).

2.3 Structure-Function Relationships

2.3.1 Homologous Enzymes and the Family of Prolidase

Homologous enzymes are related by over fifty percent sequence identity and catalyzing the same reaction on structurally similar substrates (Palmer et al., 1999). Their similarities can be explained by a common evolutionary origin. The concept of homology can group enzymes into particular enzyme families in aspect of a common evolutionary origin, so that the similarities shared in one family can be applied to a newly discovered enzyme to facilitate the understanding of its unknown properties. On the other hand, based on the fact that a protein's function is determined by its three-dimensional structure, the structure of a newly discovered enzyme should

be similar to those enzymes that share the same function. And then a three-dimensional structure model of the new enzyme can be constructed via comparison with that of the known enzymes.

Peptidases (proteolytic enzymes, protease or peptide-bond hydrolase) refer to a major class of enzymes which catalyze the proteolysis − the hydrolysis of peptide bonds. In a system proposed by Hartley (Hartley, 1960), peptidases are classified into four groups of enzymes (serine, cysteine, aspartic and metallo-peptidases) based on the catalytic mechanism of hydrolysis. The classifications were supplemented by a new group called threonine peptidases (Gerhartz et al., 2002). The catalytic nucleophiles in serine, threonine and cysteine peptidases are the hydroxyl groups serine, threonine and the sulfhydryl group of cysteine, respectively. In aspartic peptidases, the nucleophilic water molecule is bound by two aspartic amino acid residues. And in metallopeptidases, the nucleophilic water molecule is activated by one or two metal ions, which are usually chelated by three amino acid residues at the active site.

In order to reflect increasing knowledge about structures and catalytic mechanisms, a more detailed classification system called MEROPS system has been proposed by Barrett and Rawlings (Barrett, 2001). This system has three levels, in which individual peptidases comprise the basic level, and then homologous peptidases are allocated to families by comparison of amino acid sequences and finally to clans, a set of families evolved from a single ancestor. Families in the same clan are recognized by the similar folding of their peptide chains. By using this system, the amino acid sequences responsible for catalytic activity are able to be compared between peptidases in the same family since they are homologous enzymes. It is important to assign a newly-discovered peptidase to a correct family. The assignments are normally supported by the evidence of catalytic type like class-specific inhibitors, amino acid sequence data and characterizations on the purified peptidases.

2.3.2 The Classification of Prolidase

In the study of prolidsae (PepQ) from *Lactobacillus delbrueckii* subsp. *lactis* DSM7290 (Stucky et al., 1995), the computational analysis of amino acid sequence similarities revealed that

the PepQ was chiefly related to the Xaa-Pro dipeptidases (e.g., PepD of *Homo sapiens*, PepQ of *E.coli*) and Xaa-Pro aminopeptidases (e.g., PepP from *E.coli*, PepP from *Streptomyces lividans*). PepQ was proposed to have Xaa-Pro di-, or aminopeptidase activity, and the substrate specificity for Xaa-Pro gave the further evidence that it was a Xaa-Pro dipeptidase. In the aspect of its catalytic mechanism, it was found that the metallopeptidase inhibitors, EDTA and 1,10-phenanthroline, inactivated PepQ completely. Because 1,10-phenanthroline is known to chelate Zn^{2+} ions, the PepQ has been suggested as a zinc-dependent metallopeptidase. This statement was also supported by a potential zinc-binding site found in the amino acid sequence of PepQ.

Another study on PepQ of *Lactobacillus delbrueckii* subsp. *bulgaricus* B14 revealed an identity of 98% of its nucleotide sequence to the *pep*Q gene of *Lactobacillus delbrueckii* subsp. *Lactis* (Rantanen & Palva, 1997). The characterizations of PepQ of *Lb. delbrueckii* subsp. *Bulgaricus* showed that PepQ hydrolyzed almost all dipeptides containing proline at the C-terminus, and the activity of PepQ was strongly inhibited in the presence of EDTA. These properties were in accordance with the classification of PepQ as a Xaa-Pro dipeptidase.

However, Morel and his colleagues presented that the catalytic metal ions of PepQ were not only zinc in the study of a PepQ from *Lb. delbrueckii* subsp. *bulgaricus* CNRZ 397 (Morel et al., 1999). *Lb. bulgaricus* PepQ shared significant similarity with aminopeptidases P (PepPs) and methionyl aminopeptidases (PepMs) in their amino acid sequences. And the five metal ligands (Asp223, Asp234, His298, Glu237 and Glu234) constructing the active site in the PepQ sequence, were well conserved with those residues in PepPs and PepMs. These findings suggested that PepQ, PepPs and PepMs were homologous enzymes. According to the peptidases classification database ─ the MEROPS system (Barrett, 2001), *Lb. bulgaricus* CNRZ 397 PepQ was suggested to be in the M24 family of metallopeptidases, since PepPs and PepMs belong to the M24 family of metallopeptidases. Moreover, it was claimed in the same study that PepQs from *Lb. bulgaricus* B14 and *Lb. lactis* DSM7290 also belonged to the M24 family of metallopeptidases, based on the fact that the amino acid sequences only differed in one residue

between PepQ of *Lb. bulgaricus* CNRZ 397 and *Lb. bulgaricus* B14, and three residues between *Lb. bulgaricus* CNRZ 397 PepQ and *Lb. lactis* DSM 7290 PepQ.

2.3.3 Mechanism of Metallopeptidases

Since prolidase was proposed to be a metallopeptidase (Morel et al., 1999), the knowledge of the mechanism of thermolysin, which is one of the most thoroughly studied metallopeptidases, could help to understand the study of effects of structural changes on prolidase substrate specificity. Thermolysin (TLN, EC 3.4.24.27) is a Zn^{2+}-metallopeptidase, belonging to M4 family as a prototype in MEROPS classification system (Barrett, 2001). The structure of TLN has two domains, a α helical C-terminal domain and an N-terminal domain consisting of β strands (Matthews, 1988). The active site cleft is formed at the junction of the two domains with a α helix as a connection at the bottom. Four substrate binding subsites (S_2, S_1, S_1' and S_2') have been identified on this α helix in the active site cleft. Among those binding subsites, S_1' site is a hydrophobic pocket that is responsible to cleave peptide chains containing hydrophobic amino acid residues (de Kreij et al., 2001). TLN catalyzes the hydrolysis of peptide bonds containing large hydrophobic residues particularly leucine, isoleucine and phenylalanine. Two key residues Glu143 and His231 at the active site interacted with the catalytic zinc ion to catalyze the proteolysis of peptide substrates. And the major dispute was on determining whether Glu143 or His231 played the key role of a general base that deprotonated the metal-coordinated water molecule in the initial stage of the reaction (Matthews, 1988; Mock & Aksamawati, 1994). The presently agreed mechanism has been concluded and stated as following (Pelmenschikov et al., 2002). It is a single-step reaction with Glu143 playing the key role in the general base mechanism and His231 stabilizing the tetrahedral intermediate. The scheme of the mechanism of TLN catalyzed reaction is illustrated in Figure 2.3-1. In the initial state of forming the enzyme-substrate complex (ES), the zinc cation is stabilized by three ligands provided by the enzyme (His142, His146 and Glu166), and is bound to a water oxygen (O_w) and the peptide oxygen (O_p). Glu143 acts as a general base deprotonating the metal-bound water molecule for nuleophilic attack, which drives the state of ES complex to the *gem*-diolate structure (INT). At
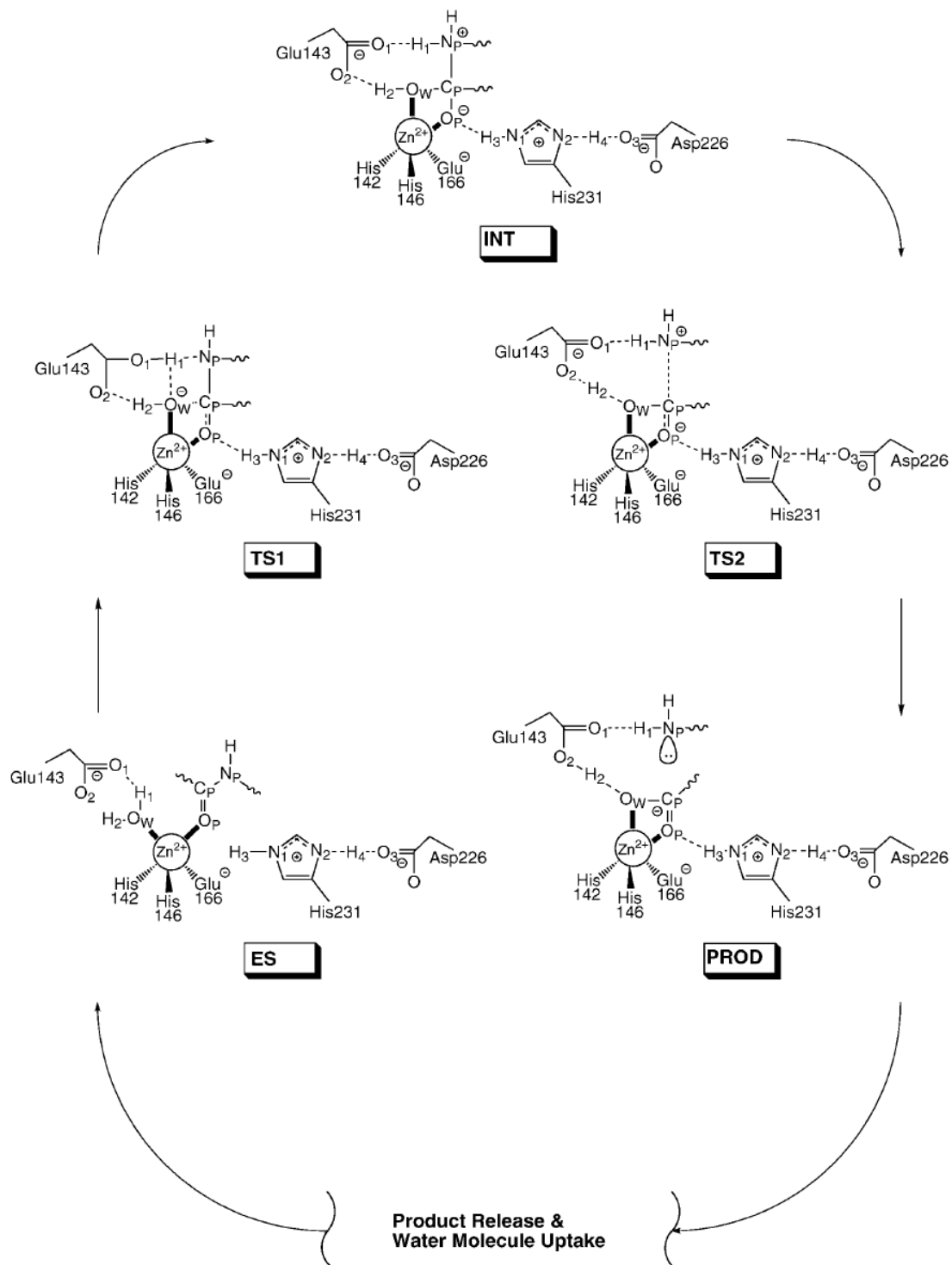
Figure 2.3-1 The scheme of the mechanism of TLN catalyzed reaction.

this state, His231 stabilizes the peptide oxygen O_p by a very strong hydrogen bond and zinc shifts the Lewis acidity strength from O_w to O_p. The collapse of INT to the products formation state (PROD) occurs relatively faster than other steps. The second proton is accepted by Glu143 from O_w to O_2 and probably transferred to the product amine. As a conclusion, TLN catalyzed reaction has the general features of the metallopeptidase mechanism, which can be considered as a general-acid-base catalysis using metal-coordinated water molecules as nucleophiles.

2.3.4 Effects of Protein Conformation on Substrate Specificity

It has been proved in many studies on structure-activity relationships of enzymes that the substrate specificity is determined by residues in the active site. One classic example is from the comparison of the substrate binding pockets of chymotrypsin, trypsin and elastase, which are serine proteases with very similar three-dimensional structures but display quite different substrate specificities (Price, 1999). These differences of substrate specificities are related to the different configurations of their substrate binding pockets. Chymotrypsin and trypsin share the same residues Gly216 and Gly226 on sides of the pocket, while elastase has Val216 and Thr226 instead of glycine. The bulky side chains of Val216 and Thr226 block the entering of substrates with bulky side chains. This explains why elastase cannot take substrates with large side chains, while the others can. The difference of the substrate binding pockets between chymotrypsin and trypsin is the residue at the bottom of the pocket, which is Ser189 in chymotrypsin and Asp189 in trypsin. Chymotrypsin shows high specificity to residues with aromatic or other large hydrophobic side chains due to the uncharged side chain of Ser189, whereas trypsin prefers residues with positively charged side chains determined by the acidic residue Asp189.

The effects of enzyme's conformation on its substrate specificity was studied in thermolysin-like proteases (TLPs), which belong to the M4 peptidase family with TLN as the prototype (de Kreij et al., 2001). The S_1' site of TLPs is composed of hydrophobic residues Phe130, Phe133, Val139, and Leu202, which are optimized for binding a smaller side chain, such as leucine, while the binding of phenylalanine is not favoured on the S_1' site. With the

expectation of an increased preference for phenylalanine at position P_1' in the substrate, De Kreij and his colleagues (2001) conducted mutations on Phe133 and Leu202, based on the criteria that these two residues together dominate the entrance of the S_1' site pocket.   Since the binding of P_1' phenylalanine is generally limited by its bulkiness compared to leucine, it is expected that enlarging of the S_1' pocket would accommodate a larger side chain.   However, the mutation of Phe133 to leucine resulted in a decreased specificity for P_1' phenylalanine substrates.   Then more attention was paid to the mutation of Leu202.   The mutations of Leu202 were done with substitutions of valine, glycine and alanine amino acids.   The alanine mutant showed more activity to substrates with a phenylalanine residue at P_1'.   This observation was explained that the alanine created more space in the S_1' pocket, while the mutant could still have enough contacts with P_1' side chain.   The mutants L202F and L202Y generated aromatic-aromatic interactions with the substrates having the P_1' phenylalanine with their newly introduced aromatic rings at the S_1 site.   As a result, the mutants L202F and L202Y increased their activities towards the substrates with the phenylalanine side chain.   In addition, the aromatic group in phenylalanine and tyrosine did not create any steric hindrance because of its parallel arrangement to the substrate according to the molecular modelling.   The L202Y mutant also had an unexpected 16-fold increase in activity towards the substrates with phenylalanine at P_1'.   This significant activity increase caused by a single mutation could be related to a hydrogen bond formed between the Tyr-OH and the substrate.

In many mutagenesis studies of proteases (Chien et al., 2004; de Kreij et al., 2001; Kadonosono et al., 2008), the substrate specificity changed due to the changes of the steric interaction and electrostatic environment at the active site or related residues by mutation-induced structural alterations.   Thus it is possible to perform mutagenesis on enzymes to alter their substrate specificities.   In this project, the proposed S_1 site of *L. Lactis* prolidase consists of Phe190, Leu193 and Val302, similar to the TLN S_1 site.   Valuable information can be derived to guide our research from the above study on how the changes of the S_1' site of TLPs affected substrate specificities.   The activity increase of the S_1' site in TLPs towards the P_1'

phenylalanine were achieved by two different strategies of mutations with concerns about the size and hydrophobicity of the S_1' binding pocket. In the investigation of the substrate specificity of *L. lactis* prolidase, the two influencing factors (*i.e.*, the steric interaction and electrostatic environment) should be considered when applying SDM on residues related to catalytic functions.

2.4 Site-Directed Mutagenesis Techniques

Amino acids in protein polypeptide chains provide functions of proteins through specific assembly of amino acids in the proteins, i.e., structures of proteins. Their structure is formed through electrostatic, such as ionic pairing and hydrogen bonding, and hydrophobic interactions. The functions of proteins include abilities to recognize specific compounds and to catalyze chemical reactions. The research to investigate the relation between function and structure is known as structure-function relationship (SFR) study.

A powerful tool in SFR studies is site-directed mutagenesis (SDM) that can remove and/or change amino acids at specific positions in proteins to analyze the roles of the specific sites.

2.4.1 Polymerase Chain Reaction (PCR) Based Methods

Since the incorporation of polymerase chain reaction (PCR) allows high-efficiency mutagenesis in a fairly short period of time, PCR-based methods have gained popularity and thus received a lot of developments.

One of the widely used PCR-based protocols is the QuikChange^{TM} Site-directed Mutagenesis System (QCM) designed by Stratagene (La Jolla, CA, USA) (Wang W, 1999), which is employed to complement all the mutations in this thesis. It is a widely used PCR-based approach using a high fidelity DNA polymerase, *Pfu* DNA polymerase, and two complementary primers containing desired mutations. The principle of this method is using two complementary primers to amplify the entire plasmid in a single PCR reaction. The PCR-generated plasmids are negatively selected by the digestion of methylated parental plasmids with the *Dpn*I treatment, and then transformed into a mismatch repair-defective strain of *E.coli*.

The whole procedure is featured by its rapid and reliable operation, and high efficiency of the desired mutagenesis, which is normally in the range of 70~90%. However, this method is limited to small primer size of 25~45 bases and the introduction of up to five base alterations. These limitations will be taken into consideration when designing the pair of complementary primers. This method allows the mutation with high efficiency in as short as 24 hours.

However, the primer-dimer formation is more favourable compared to the primer-template annealing when the longer primers are used in this method. To overcome the limitation of the primer length in the standard QCM, a modified two-stage PCR mutagenesis protocol has been developed (Wang W, 1999). The strategy of this method contains two stages of performing the two extension reactions of forward and reverse primer in separate tubes and subsequently carrying out the standard QCM procedure on the mixture of these two reactions. The separated manipulation of two primers' annealing in the first stage not only can avoid the primer-dimer formation, but provides a perfect match of primers to the newly synthesized template plasmids from the first stage thus improves the efficiency of mutagenesis.

Recently, a simplified method is described in Shenoy's method (Shenoy & Visweswariah, 2003) by using a single mutagenic primer and incorporating *Dpn*I digestion to remove the methylated parental DNA thus raise the mutation efficiency. Also a method was described to contain two rounds of *ds*DNA synthesis with a phosphorylated mutagenic primer and a universal primer with the combination of *Dpn*I digestion (Xin et al., 2004). By using the T4 DNA polymerase and ligase, this method can overcome the error rate and limitation of product's size caused by using *Taq* DNA ligase in PCR-based SDM.

2.4.2 Strategies of Using Site-Directed Mutagenesis

SDM introduces mutations using an oligonucleotide that has a mutated sequence. By *in vitro* synthesis of a DNA molecule, the oligonucleotide is incorporated into a target gene, yielding a mutated gene. Two general strategies of the SDM are employed to analyze the enzymatic activity and other properties: substitution and deletion.

As strategies of the substitution, there are two ways commonly used. One strategy is to

replace a potential catalytic residue directly determining the enzymatic activity by other amino acids to see if it would cause the loss of function.   However, one can only confidently claim that the residue replaced is essential for the enzymatic activity when the loss of function is caused by SDM without significant disruption of the conformation of the enzyme.   An example of the above way of substitution was provided by the study on the structure-function relationship of porcine pepsinogen (Lin et al., 1989).   The active site residue Asp32 was changed into an Ala residue by the SDM.   Then it was found that the D32A mutated pepsinogen was no longer converted to pepsin under acid conditions, indicating that intramolecular pepsinogen activation was accomplished by the pepsin active site.   The second strategy of substitution is to change the residues that have interactions with the catalytic residues into a different amino acid.   Changes made to these residues usually do not result in the total loss of function.   Instead they affect the enzymatic activity by motivating the conformational changes on catalytic residues.   In a study (Lin et al., 1992), the Ser35 was changed to an alanine to analyze the ionization property of porcine pepsin.   In this aspartic peptidase, Ser35 is located closely to Asp32, one of two catalytic residues.   It was argued whether this serine provided a hydrogen bond to the carboxyl group of Asp32 to lower the pK_a values of the catalytic group.   However, the mutant S35A had no significant effect on pK_a values and catalytic activity.   These results indicated that hydrogen bonds from Ser side chains should not lower the pK_a values significantly more than do water molecules.

There are more strategies introduced using SDM other than the two concepts above, for example, the usage of SDM to investigate the contribution of certain amino acid residues to the substrate specificity by changing selected residues to other amino acids.   In the research of the influenza A virus neuraminidase (NA) (Kobasa et al., 1999), SDM on residue 275 near the enzymatic active site of NA demonstrated that the change of isoleucine to valine resulted in higher NeuAcα2-6Gal activity without influencing NeuAcα2-3Gal activity (NeuAcα2-6Gal and NeuAcα2-3Gal are *N*–acetylneuraminic acids bound to galactose through an α2,6 linkage and α2,3 linkage respectively).   Residue 275 was adjacent to Glu276 and Glu277, both of which are

directly involved in the binding of sialic acid to the active site.   It was explained that the raised NeuAcα2-6Gal activity was due to the decreased restrictions on accessibility to the active site by altered side chain of residue 275.   Moreover, the deletion strategy helps to identify a critical region in an amino acid sequence by removing single or several amino acid residues.   A series of deletion mutations have been done in the transmembrane domain of the Sindbis virus glycoprotein (E2) in order to identify a region critical for virus growth (Whitehurst et al., 2006). They found that single deletions located closer to the cytoplasmic of the membrane bilayer had a more deleterious effect on virus growth and infectivity than deletions located closer to the luminal of the membrane bilayer.   And an eight amino acid deletion in the C terminal region of the E2 transmembrane domain demonstrated the vital function of this segment in normal virus production.

2.5 Allosteric Behaviours

Wild type prolidase from *L. lactis* NRRL B-1821 displays the deviation from Michaelis-Menten kinetics.   The wild type showed a sigmoid curve in the plot of enzyme activities against substrate concentrations.   This observation demonstrates that wild type prolidase exhibits allosteric behaviour (Yang & Tanaka, 2008).

2.5.1 Allosteric Enzymes

Many enzymes exist as oligomers composed of distinct subunits rather than a single peptide chain.   The subunits are often identical with one catalytic site per subunit (Traut, 2008a).   If the binding of substrate on one catalytic site does not affect the binding properties on other sites, such enzyme subunits are said to be independent and non-cooperative.   However, there are oligomeric enzymes that are able to be regulated by ligands bindings, and this behaviour is designated allosteric behaviour or cooperativity.

Allosteric enzymes are distinguished from non-allosteric enzymes essentially in the context of conformational states.   All enzymes have multiple conformations under physiological conditions (Traut, 2008a).   A non-allosteric enzyme usually adopts only one conformation as the

active state with the others being inactive state, and the population of the active conformer is never changed by any ligand binding. An allosteric enzyme has two conformational states, R (relaxed state), representing the active form, and T (tense state), being the inactive form. In the absence of any ligands, the majority of the population is in the T state, which is at a lower energy state. When substrates or activators become sufficient, these ligands would bind to enzyme molecules in the R state, increasing the abundance of this state thus to raise the enzyme activity. Therefore, the allosteric regulation or the cooperativity of activity is performed by changing the distribution of the enzyme molecules between the two active and inactive conformational states via different ligand-bindings.

2.5.2 Kinetics of Allosteric Enzymes

Enzymes without the cooperativity follow the Michaelis-Menten kinetics shown as $v = V_{max} \cdot S/(K_m+S)$, and generate a hyperbolic velocity curve (Figure 2.5-1). This equation implies that i) enzymes show first-order kinetics at low substrate concentrations, ii) enzyme reaction rates do not go beyond V_{max} even at extremely high substrate concentrations, and iii) the dissociation constant is K_m that equals to the concentration where the enzyme shows a half of V_{max}. The enzyme kinetics based on this relation is called the Michaelis-Menten kinetics. Many properties of enzymes can be explained using this kinetics, such as the affinity of the substrates. Therefore the Michaelis-Menten kinetics is widely recognized as a powerful tool for enzyme analyses.

Allosteric enzymes, however, do not follow the Michaelis-Menten kinetics, and the kinetic plots for them yield sigmoidal curves (Figure 2.5-2). While the Michaelis enzymes have constant affinity, the allosteric enzymes show two different affinities at R and T states, which are represented by K_R and K_T, respectively. However these two affinity constants cannot be extracted from the sigmoidal curve for an allosteric enzyme in the same manner for a hyperbolic curve. Instead, a putative affinity constant $K_{0.5}$ is defined as the substrate concentration at 1/2 V_{max}. Then the allosteric behaviour can be described in the Hill equation
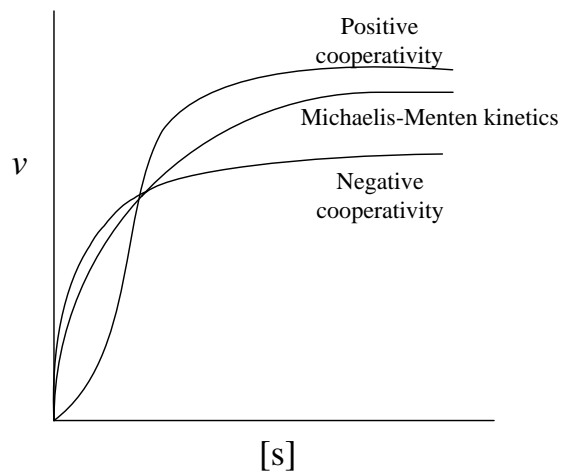
Figure 2.5-1 The kinetic plots of velocities versus substrate concentrations.
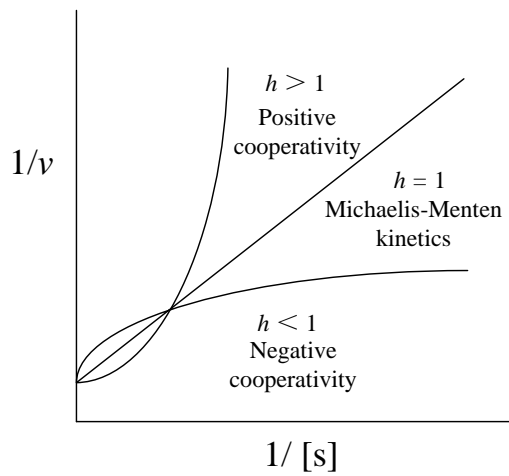
Figure 2.5-2 The Hill plots of Michaelis-Menten kinetics, positive and negative cooperativities.

(Equation 2.1). *h* is the Hill constant, which represents an index of cooperativity. If $h = 1$, there is no cooperativity; if $h > 1$, there is positive cooperativity; if $h < 1$, then there is negative cooperativity.

$$v = \frac{V_{max}S^h}{K_{0.5} + S^h}$$ (Equation 2.1)

In the case of positive cooperativity, the enzymes are more sensitive to the changes of substrate concentrations at low concentrations than the non-cooperative enzymes are. In other words, smaller changes of substrate concentration are required to reach 90% of the maximum velocity from the 10%. The enzyme with positive cooperativity shows lower activities than non-allosteric enzyme at low substrate concentrations (Figure 2.5-1). These depressed activities are influenced by the abundant T state at the initial stage of the reaction, whose low affinity (K_T) determines the lower activity. After the R state prevails over the T state via substrates or activator binding to some extent, the activity drastically increases.

In contrast, the negative cooperativity weakens the response to the changes of substrate concentration, requiring more substrate concentration changes to reach 90% of the maximum velocity. As shown in the double reciprocal plot of enzyme activities and substrate concentrations (the Lineweaver-Burk plot) (Figure 2.5-2), the concave and convex curves represent the positive and negative cooperativity, respectively, with changing slopes compared to the constant slope K_m/V_{max} in Michaelis-Menten kinetics.

In a practical way to determine the allosteric behaviour, the initial velocities at several substrate concentrations are measured to plot the velocities of enzyme activity against substrate concentrations for the double reciprocal plot. The Hill constant is calculated by fitting the plotted curve into the Hill equation (Equation 2.1) to determine whether the enzyme has cooperativity, and positive or negative cooperativity.

2.5.3 Aspects in Conformational Changes in Cooperativity

Allosteric enzymes usually stay in the T state without binding to ligands. Once the cooperativity is triggered by ligands binding, a slight conformational change is required to

transform the catalytic site to the R state conformation.   Three possible mechanisms for conformational changes have been established (Traut, 2008b).   (i) In smaller proteins, the catalytic site normally forms at the junction of two domains, which are usually connected by a short but flexible polypeptide segment.   A little conformational change of the catalytic site can thus be easily achieved by rotation of one domain relative to the other.   (ii) The catalytic pocket is usually formed across the interface between the subunits in oligomeric enzymes.   The dissociation of the two subunits would enlarge the catalytic pocket residing at the dimer interface. The change of enzyme activities would be a function of states of oligomeric subunits.   (iii) Also in oligomeric enzymes, there is another type of the association of domains, so-called "3D domain swapping".   The catalytic pocket is composed of domains from separate protein subunits. Usually the interactions between domains from neighboring subunits determine the conformational changes of the function unit.

2.5.4 Positive Cooperativity in the Metabolism

A specific metabolic pathway involves different enzymes in a sequential way for the synthesis of a single end product, and several pathways are connected together to supply a certain nutrition pool, in which the amount of each end product may be manipulated by dedicated regulations of allosteric regulatory enzymes in the pathways.   These enzymes perform regulations in various ways according to their intrinsic types of cooperativity.   Since the *L. lactis* prolidase has been reported to show positive cooperativity (Yang & Tanaka, 2008), the significance of the positive cooperativity for the metabolism is interested.   Positive cooperativity enables enzymes to be more sensitive to changing concentrations of the specific cellular metabolites that they recognize, thus to response to the environmental conditions by appropriately altering their activity.   These regulations make the metabolic pathway process in a control pace.   The allosteric behaviour of the *L. lactis* prolidase shown to its substrates (Yang & Tanaka, 2008) implies that the prolidase responses sensitively to the changes in the dipeptides supply, and thus to have a regulatory role in the nitrogen metabolism.

2.6 Substrate Inhibition

2.6.1 Substrate Inhibition of Prolidase

The previous study in Dr. Tanaka's lab revealed the existence of substrate inhibition in wild type prolidase (Yang & Tanaka, 2008).   Substrate inhibition is to describe the phenomenon that the enzyme activity is totally depressed or simply reduced at sufficient high concentration of the substrate.   It can be envisioned as competitive mechanism, and is achieved by two molecules of substrate simultaneously bind to the active site of E (enzyme) simultaneously forming inactive ESS complex (Parkin, 2003).

Since *L. lactis* prolidase possesses the allosteric behaviour, the substrate inhibition could be raised from the binding of substrate either at an inhibitory second site (heterotropic allostery) or at the active site (homotropic allostery).   The possibility of heterotropic allostery inhibition was first suggested in the study aspartate (Heyde, 1976), which demonstrated a second binding site for dicarboxylic acids near the active site to inhibit the enzyme activity.   And the homotropic allostery was postulated by Licata (LiCata & Allewell, 1997), who argued that the substrate inhibition of aspartate transcarbamylase (ATcase) was a consequence of its allosteric behaviour based on the fact that ATcase exhibited positive cooperativity in low substrate concentration and consequently its activity was reduced by sufficient high substrate concentration.

According to the *v-S* plot of wild type prolidase obtained in previous studies, the curve was sigmoidal in the range of low substrate concentrations, indicating the presence of allosteric behaviour.   Then the substrate inhibition was displayed at substrate concentrations of greater than 4 mM.   These observations were in accordance to the homotropic allostery of substrate binding.   This kind of allostery can be visualized as one molecule of substrate binds to the active site with its side chains binding to their corresponding subsites.   In case of substrate inhibition, each subsite was occupied by a side chain from different substrates, resulting in the formation of a nonproductive ESS complex (Parkin, 2003).

2.6.2 Kinetics of Substrate Inhibition

According to the description of the homotropic inhibition mechanism that two molecules of

S (substrate) form a nonproductive ESS complex at the active site of E, the inhibition can be expressed in a model (Equation 2.2) with a dissociation constant (K_i) for the inhibited enzyme species (ESS).   And the enzyme reaction velocity can be calculated by Equation 2.3.

$$E + 2S \xrightleftharpoons{K_i} ESS \qquad \text{(Equation 2.2)}$$

$$v = \frac{V_{max} \cdot S}{K_m + S + \dfrac{K_m S^2}{K_i}} \qquad \text{(Equation 2.3)}$$

2.7 The pH Dependency of Protein Activity

The enzymes in general show different levels of activities in a limited pH range, and most exhibit bell-shaped profile of pH dependence with optimum pH at which their activities achieve the maximum.   This dependence of enzyme activity on pH relates to the ionization of the titratable groups in enzyme active site and also in the substrates.

The common titratable groups in proteins include the C-terminal carboxyl, carboxyl groups of aspartic and glutamic acids, the imidazole group of histidine, the sulfhydryl group of cysteine, the amino group of lysine and arginine, the hydroxyl group of tyrosine and the N-terminal amino group (Harris & Turner, 2002).   At a certain pH, a titratable group is either in protonated or deprotonated form determined by its apparent pK_a value in the protein.   When the pH is higher than its apparent pK_a value, the titratable group would be deprotonated.   For the group to be protonated, the pH needs to be lower than its apparent pK_a value.   A titratable group's apparent pK_a value is different from its intrinsic pK_a value in aqueous solution due to the microenvironment created around it by the protein.   In other words, the intrinsic pK_a value of a titratable group is driven to its apparent pK_a value by the charge-charge or charge-dipole interactions with fully or partially charged groups, respectively, that surround it.

In the case of charge-charge interactions, two neighbouring groups with the same negative charge will increase each other's pK_a value, facilitating the protonation in environmental pH to avoid like-charge repulsion (Harris & Turner, 2002).   If the neighbouring groups are both protonated with positive charge in environmental pH, then the pK_a value of the catalytic group

will be decreased to make the deprotonation easier against the repulsion. If the neighbouring groups have opposite charges, then the pK_a value of positively charged group will always get higher and that of negatively charged group will get lower to favour the opposite-charge attraction.

The titratable group can also have charge-dipole interactions with partially charged polar residues. And normally the charge-dipole interactions are presented by the formation of hydrogen bonds. The energy generated by the formation of a hydrogen bond is utilized to increase the pK_a value of the hydrogen bond donor and meanwhile decrease the pK_a value of the hydrogen bond acceptor, facilitating an even stronger hydrogen bonding.

The interactions in the microenvironment around the catalytic group can be investigated by mutations at or near the enzyme active site. This kind of research was early reported with the subtilisin from *Bacillus amyloliquefaciens* (Thomas et al., 1985), and recently performed on TLN (Kusano et al., 2006), *Saccharomyces cerevisiae* phosphoenolpyruvate (PEP) carboxykinase (Yevenes et al., 2006) and α-amlyase from *Bacillus licheniformis* (Lee et al., 2006).

A study of TLN is taken as an example to demonstrate the charge-charge interactions, in which the pH dependence of the enzyme's activity was affected by the SDM on amino acid residue Asn112 located closely to the catalytic zinc and catalytic residues Glu143 and His231 at the active site of TLN (Kusano et al., 2006). The replacement of residue Asn112 to the anionic residue aspartate was observed to endow TLN with a different profile of pH dependency and change its pK_a from 5.3 to 5.7. As discussed before, the increase of pK_a value (by 0.4 units) should relate to the charge-charge interaction of the negative charged residue Asp112 with a neighbouring catalytic group possessing the same charge. Asp112 was proposed to interact with the anionic catalytic residue Glu143 or the zinc-bound hydroxide ion Zn^{2+}-OH, thus its protonation should be stabilized to avoid the like-charge repulsion. Therefore, it was concluded that a different pH-dependence profile of the N112D mutant compared to that in wild-type TLN was attributed to the increased pK_a value of the mutant generated by the charge-charge interactions among the neighbouring functional groups.

Besides the charge-charge interaction, an example for charge-dipole interaction was found in the mutagenesis study of *Saccharomyces cerevisiae* PEP carboxykinase. This study suggested that the affinity of PEP carboxykinase for Mn^{2+} depends on the deprotonation of a key residue Lys213, and evaluated the role of neighbouring residue Phe416 by mutating it to polar residue tyrosine. This mutation was demonstrated to be unfavourable upon the observation that the affinity of PEP carboxykinase for Mn^{2+} became lower. Also based on the measured increase of the pK_a of Lys213 by 1.5 pH units, it was indicated that the introduced polarity triggered the charge-dipole interaction between Lys213 and Tyr416, resulting in the protonation of Lys213. For the appropriate Mn^{2+} binding, Lys213 should be always in the neutral form. So the hydrophobic residue Phe416 provided a low polarity microenvironment maintaining Lys213 in the neutral form to allow suitable Mn^{2+} binding.

The above discussions suggest that the changes of pH dependence of enzyme activities can be explained by the different pK_a values that are introduced by the mutations of catalytic residues.

2.8 The Thermal Dependency and Stability of Protein Activity

For many enzymes, the conformational motion plays a vital role in enzyme activity, which can be interpret in two aspects: the stability of the structure for being recognized by the approaching substrates; and the flexibility of the structure for being able to be transformed when releasing the products (Hammes-Schiffer, 2002). These two contrary requirements for enzyme activities result in a minimum activation energy when the enzyme's physiological temperature is achieved, which is also considered as its optimum temperature. And the overall conformational flexibility of enzymes should be preserved at their optimum temperatures, according to the theory of "corresponding states" (Jaenicke & Závodszky, 1990). For example, the glyceraldehyde-3-phosphate dehydrogenase (GAPDH) from *Thermotoga maritime* (TmGAPDH), which was a thermostable enzyme with optimum temperature near 68°C, was found to be more rigid at room temperature than its mesophilic counterpart GAPDH from rabbit muscle (RmGAPDH) with optimum temperature of 25 °C (Hajdú et al., 2008). And the largest structural differences were observed in flexibility at the NAD binding and substrate binding

regions in TmGAPDH and RmGAPDH.   These findings indicated that thermal dependences of enzyme activities closely relied on the conformational flexibility of the regions being vital for enzyme functions, and enzymes preserved the maximum conformational flexibilities at their optimum temperatures.

Based on the above discussions, it is conceivable that changes in conformational flexibility of the functional regions are able to cause the different thermal dependences of enzyme activities, specifically their optimum temperatures.   A study on a lysozyme is taken as an example to elucidate the effects of the conformational changes on the thermal dependency of enzyme activity by mutations of Met12 and Leu56 in the wild type (Yoshida et al., 2005).   The thermal dependency of the activity was examined in M12L/L56F mutant with double alterations of Met12 and Leu56 to leucine and phenylalanine respectively.   Compared with that of the wild type activity, the M12L/L56F mutant had optimum activity at a higher temperature.   In the well-elucidated crystal structure of the wild-type lysozyme, a cavity is formed far from the active site by a surrounding hydrophobic core, which consists of residues Leu8, Met12, Leu17, Trp28, Ile55, Leu56, Ile88 and Val92.   The residues Met12 and Leu56 face each other across the cavity without van der Waals interactions.   Due to the fact that the cavity was far away from the active site, the shift of optimum temperature in the M12L/L56F mutant was caused by long-range effects rather than by the direct pK_a changes of catalytic residues.   They suggested that the replacements of Met12 and Leu56 by residues leucine and phenylalanine stabilized the cavity, thus restricted the internal motions of the mutant compared to the wild type.   In other studies, the internal motion was reported to be critical for the enzyme activity due to the observed conformational dynamics of the active site, *i.e.* suitable relaxation of the conformational rigidity was required for enzyme function (Cole & Loria, 2002; Falzone *et al.*, 1994).

In contrast, the requirement of enzyme activity for the internal motions is adverse to the conformational rigidity, which is critical for the enzyme stability.   Proteins fold to minimize their free energy, and the stable state is to have hydrophobic residues well packed inside and hydrophilic residues at the surface.   However, the enzyme stability was increased by the

introduction of hydrophobic amino acids to the solvent-exposed surface residues in TLN, such as residue 63 (Van den Burg et al., 1994) and residues 128 and 225 (Tatsumi et al., 2007).   These phenomena were interpreted that the tightly packed hydrophobic surface residues formed a layer separating the hydrophilic protein surface and solvent from the rest of protein, thus stabilizing the three-dimensional structure of the enzyme through preventing the invading of water molecules and unfolding process.

A relationship between enzyme stability and activity was described based on the study of mutations at the active site of T4 lysozyme (Shoichet et al., 1995).   It was generally stated that residues in an enzyme participating in catalysis were not optimized for stability.   This statement was supported by several observations in research of enzymes: Thermophilic enzymes with higher stability always have lower activities than their mesophilic counterparts at low temperatures; And the protein engineering designed to elevate enzyme activity is always accompanied by the destabilization of the enzyme (Eriksson et al., 1992; Scrutton et al., 1992).

2.9 The Metal Dependency of Prolidase Activity

According to the MEROPS classification system, prolidase belongs to the M24 family of metallopeptidases (Morel et al., 1999), of which the catalytic mechanism involves metal ions. The major function of metal ions is generally suggested to act as lewis acids coordinating with the substrate peptide carbonyl oxygen to facilitate the nucleophilic attacks (Lipscomb & Strater, 1996; Matthews, 1988).   A water molecule is employed as the nucleophile by many metallopeptidases, such as TLN (Matthews, 1988) and metallo-β-lactamases (Badarau & Page, 2006).   And the metal ion coordinates to the water molecule in an intermediate anion of metal and hydroxide ion (M^{2+}-OH).   If the pK_a of metal-bound water gets lower, then the metal ion center would have more electron deficiency to be a better Lewis acid to stabilize the negative charge generated on the substrate peptide carbonyl oxyanion during the nucleophilic attack, thus to accelerate the catalytic reaction.   Likewise, a higher pK_a of metal-bound water indicates that the metal ion acts as a weaker Lewis acid resulting in a decreased enzyme activity.   This increase in enzyme activity with lower pK_a of metal-bound water can be also explained as the

stabilization of the intermediate anion by metal ion acting as a better Lewis acid stabilizing the negative charge during catalytic reaction. However there are cases that enzyme activity increases with higher pK_a of metal-bound water, indicating that the nucleophilic role of metal-bound hydroxide ion is more important than the coordinating role for developing a more electron deficient metal ion center during nucleophilic attack.

Substitution of the native metal ion by other metal ions provides a pathway to look into the relationship between the enzyme activity and the pK_a of metal-bound water. Badarau et al. have studied on metallo-β-lactamases (Badarau & Page, 2006) by replacing the native catalytic zinc ion with cadmium (II) in this aspect. The pK_a of the Cd^{2+}-bound water was measured to be about three pH units larger than that of the Zn^{2+}-bound water. And the native metallo-β-lactamases with Zn^{2+} was demonstrated to have higher activity than the enzyme substituted of Cd^{2+}. According to the above discussion on the role of metal-bound water, these observations suggested that the increase of pK_a of Cd^{2+}-bound water reduced the electron deficiency of the metal ion center, leading to lower stabilization of the negative charge developed on the substrate peptide carbonyl oxyanion during nucleophilic attack. The enzyme activity was more related to the role of metal ion as a Lewis acid than a nucleophile.

3 HYPOTHESES and OBJECTIVES

Three residues Phe190, Leu193 and Val302 of *L. lactis* prolidase were proposed by Yang and Tanaka (2008) to compose the S_1 substrate binding subsite, and their hydrophobicity was suggested to determine prolidase's preferences to hydrophobic substrates.   Based on their initial findings, it was hypothesized in this study that the mutations on these S_1 residues would alter the substrate specificity of prolidase by introducing charged amino acids to the S_1 site.   The mutations at these three positions might also influence prolidase's unique property of allosteric behaviour, based on the concern that the allosteric determining residue Arg293 was located closely to Val302 (Zhang et al., 2009).

Following the above hypotheses, several studies have been designed and implemented to investigate the characteristics of mutated prolidases as well as the wild type, including substrate specificity, pH dependency, allosteric behaviour and substrate inhibition, thermal dependency and metal dependency.   The objectives of this project are: to analyze the effects of substituted hydrophilic functional groups on prolidases' substrates specificity, pH and thermal dependency, and allosteric behaviour; to find which residue(s) is more important among Phe190, Leu193 and Val302 residues at the S_1 site for determining wild type prolidase's catalytic efficiency, substrate binding or allosteric behaviour.

4 MATERIAL and METHODS

4.1 Site-Directed Mutagenesis

The pUC18 clones of *L. lactic* prolidase NRRL B-1821 (ARS culture collection, USDA, Peoria, IL, USA) were constructed in Dr. Tanaka's lab (Yang & Tanaka, 2008). They were cultivated and the plasmids were isolated to use as *ds*DNA templates for SDM.

Considering the hydrophobicity, charges and sizes of amino acid residues, three residues, Phe190, Leu193 and Val302, were chosen for single amino acid mutations in the S_1 site of *L. lactis* prolidase: Phe190 was changed to glutamate, arginine or threonine (F190E, F190R, and F190T, respectively); Leu193 was changed to glutamate, arginine or threonine (L193E, L193R, and L193T, respectively); Val302 was changed to aspartate, lysine or threonine (V302D, V302K, and V302T, respectively). After determining the substrate specificity profiles of all nine mutants on single residues, the combined mutations on two amino acid residues, Leu193 and Val302, were selectively performed. The combined mutations were: the mutant of Val302 to aspartate together with Leu193 to glutamate (L193E/V302D); and the mutant of Val302 to aspartate together with Leu193 to arginine (L193R/V302D). These two combined mutations were implemented by the introductions of mutagenic oligonucleotide primers, L193R and L193E, respectively, to the pUC18 clone of the V302D mutant prolidase gene. Pairs of corresponding complementary mutagenic oligonucleotide primers were designed as following:


```
F190E-F
5'-CAC AgA TgT CAg Agg ACA CAC TAg TTT TAT CAg-3'
                            BcuI


F190E-R
5'-CTg ATA AAA CTA gTg TgT CCT CTg ACA TCT gTg-3'
```

F190R-F
5'-CAC AgA TgT CTC gCg ACA CgC TTg-3
                Bsp68I

F190R-R
5'-CAA gCg TgT CgC gAg ACA TCT gTg-3'

F190T-F
5'-CAC AgA TgT CgA CTg ACA CgC TTg-3'
                SalI

F190T-R
5'-CAA gCg TgT CAg TCg ACA TCT gTg-3'

L193E-F
5'-CAT TTg ACA Cgg AAg TAC TAT CAg gAg CTC-3'
                        ScaI

L193E-R
5'-gAg CTC CTg ATA gTA CTT CCg TgT CAA ATg-3'

L193R-F
5'-CAT TTg ACA CgC gTg TTT TAT C-3'
                MluI

L193R-R
5'-gAT AAA ACA CgC gTg TCA AAT g-3'

L193T-F
5'-CAT TTg ACA CgA CAg TAC TAT CAg gAg CTC-3'
                         ScaI

L193T-R
5'-gAg CTC CTg ATA gTA CTg TCg TgT CAA ATg-3'

V302D-F
5'-Cgg AAT ggA TgA TCA CgA ATA TCC-3'
                BclI

V302D-R
5'-ggA TAT TCg TgA TCA TCC ATT CCg-3'

```
V302T-F
5'-Cgg AAT ggA CAC TCA TgA ATA TCC ATC-3'
                    PagI


V302T-R
5'-gAT ggA TAT TCA TgA gTg TCC ATT CCg-3'


V302K-F
5'-ggA ATg gAC AAg CAC gAA TAT CCA TCg ATT gTT gCC-3'
                                    Bsu15I


V302K-R
5'-ggC AAC AAT CgA Tgg ATA TTC gTg CTT gTC CAT TCC-3'
```

The newly introduced restriction enzyme sites were indicated by underlines and the name of restriction enzymes. Designed primers were then synthesized at Integrated DNA Technologies (IDT), Coralville, IA, USA.

The single and combined mutations and protein expressions were carried out using the technique of QuikChange™ SDM in PCR (Wang W, 1999). The total 100 μL reaction mixture of PCR contained 1 μg of template plasmid (the pUC18 prolidase clone), 20 pmol of each complementary primer, 0.02 mM dNTPs (Roche, Basel, Switzerland) and 1 unit of *Pfu* DNA polymerase (Fermentas, Burlington, ON, Canada). PCR was carried out with 16 cycles, consisting of 1 min denaturation at 95°C, 1 min primer annealing at 55°C and extension at 68°C of increasing duration by 5 sec per cycle from 3 min 30 sec to 4 min 45 sec.

The PCR product was then treated with *Dpn*I (Fermentas, Burlington, ON, Canada) to digest the methylated parental template DNA. The treated products were transformed into *E.coli* TOP10F' and cultivated on the LB (pH 7.5) agar (1.5%) plate with 150 μg/mL ampicillin. The grown colonies on the plate were cultivated in 2 mL LB broth and plasmid DNA was isolated using the alkali-SDS DNA preparation method (Brown, 2001). The mutants were screened by restriction endonuclease digestion of isolated plasmids. The recipe of restriction endonuclease reaction mixture is 1 μg isolated plasmid and 1 unit restriction enzyme (Fermentas, Burlington, ON, Canada) corresponding to the introduced restriction site of the mutant plasmids. The

digested plasmids were analyzed on an agarose gel electrophoresis if they have expected fragment sizes. The positive mutants were further confirmed by DNA sequencing at the National Research Council-Plant Biotechnology Institute (Saskatoon, SK, Canada).   Then the sequencing results were validated to the correct nucleic acid sequences using the BLAST database in the PubMed online services.   The confirmed recombinant *E.coli* cells containing mutated pUC18 plasmids were stored as glycerol solutions at -70°C.

The pUC18 clones yielded the mutants easily by its high replication number, but it was hard to get significant amount of mutated protein because of its poor expression efficiency.   In order to gain high expression of mutated prolidases, the mutated prolidase genes from the pUC18 clones were subcloned into pKK223-3 plasmids for protein expressions.

To subclone to pKK223-3 plasmids, the mutated prolidase gene was firstly amplified by PCR using *Pfu* DNA polymerase and two primers (LacQ (C-2): 5'- ATT CTG CAG TTA GAA AAT TAA TAA GTC ATG - 3', LacQ (N-2): 5'- GGA GAA TTC ATG AGC AAA ATT GAA CGT ATT - 3'. IDT, Coralville, IA, USA) that are designed to amplify the gene with an introduction of *Eco*RI and *Pst*I restriction site at N- and C-terminal, respectively.   The PCR products were then digested by *Dpn*I, *Eco*RI and *Pst*I to exclude methylated parental DNA and to form the adhesive ends.   The amplified mutant gene DNA underwent ligation with *Eco*RI-*Pst*I-digested pKK223-3 plasmids using T4 DNA ligase (Invitrogen, Carlsbad, CA, USA).   Then the recombinant pKK223-3 plasmids were transformed into *E.coli* TOP10F' and grown on the LB-Agar plate with ampicillin.   The plasmids were isolated from the culture of the grown colonies and checked on the agarose gel after *Eco*RI and *Pst*I digestion for mutants.   The positive pKK223-3 clones were identified to yield 1.0 and 4.6 kb fragments on the agarose gel electrophoresis.   The positive pKK223-3 clones were further verified by DNA sequencing at the National Research Council-Plant Biotechnology Institute (Saskatoon, SK, Canada).

The recombinant *E.coli* carrying pKK223-3 clones with desired mutations were preserved as glycerol solutions at -70°C for further expression and characterization of mutated prolidases.

4.2 Expression of Mutated Prolidase

The expression of mutated prolidases followed the standard procedure (Yang & Tanaka, 2008). The recombinant *E.coli* containing desired mutated prolidase was cultivated in total 300 mL LB broth (pH 5.5) containing 150 µg/mL ampicillin in 16°C waterbath with agitated shaking, and induced at optical cell density of 0.5 with IPTG (Invitrogen, Carlsbad, CA, USA) and chloramphenicol of 1 mM and 1 µg/mL final concentration, respectively. It was noticed that good aeration was crucial to the cells growth and high expression of *L. lactis* prolidase. In practice, the mutated prolidase was cultivated in a 500 mL flask containing 50 mL media, and six flasks of this culture were gathered to get 300 mL final culture of each mutated prolidase.

4.3 Purification of Prolidase

The cells were resuspended in 10-times volume/wet cell weight of a 20 mM sodium citrate (pH 6.0)/ 1 mM $ZnCl_2$/ 50 mM NaCl solution. The resuspended cells were disrupted using ultrasonication. After centrifuge to remove cell debris (Sorval ss-34, 12,000 rpm, 20 min, 4°C), the crude extracts were brought to 40 % saturated ammonium sulfate and kept on ice for 12 h. The precipitated protein fractions were removed by centrifuge (Sorval ss-34, 12,000 rpm, 20 min, 4°C). The supernatant was then brought to 60 % saturated ammonium sulfate and kept on ice for another 12 h. The precipitant was collected by centrifuge (Sorval ss-34, 12,000 rpm, 20 min, 4°C), and was dissolved in a 2 mL buffer solution (20 mM sodium citrate (pH 6.0)/ 1 mM $ZnCl_2$/ 50 mM NaCl). Then the partially purified sample was dialyzed against 4 L of 20 mM sodium citrate (pH 6.0)/ 1 mM $ZnCl_2$. The protein concentration of the dialyzed protein fraction was determined and protamin sulfate was added at 10 % of the total protein amount. The mixture was kept at 4°C for 12 h and centrifuged (Sorval ss-34, 12,000 rpm, 20 min, 4°C) to remove nucleic acid fractions. The supernatant was applied onto a DEAE Sephacel column (2.5 ϕ × 20 cm, GE Health Sciences, Little Chalfont, Buckinghamshire, UK) equilibrated with 20 mM sodium citrate (pH 6.0)/ 1 mM $ZnCl_2$. Prolidase was eluted using a linear gradient from 0 to 0.5 M NaCl. Prolidase fractions were identified on SDS-PAGE and concentrated with Amicon YM-10 ultrafiltration (Millipore, Billerica, MA, USA). The condensed sample was again

loaded on a Phenyl Sepharose column (1.5 ϕ × 20 cm, GE Health Sciences, Little Chalfont, Buckinghamshire, UK) equilibrated with 20 mM sodium citrate (pH 6.0)/ 1 mM ZnCl$_2$/ 1 M ammonium sulfate. An ammonium sulfate solution with gradually decreasing concentration from 1 to 0.2 M was applied to the column to obtain the eluted fractions. Then the fractions containing prolidase were identified on SDS-PAGE and condensed with Amicon YM-10 ultrafiltration. The concentrated sample was kept at -20°C as a 50 % glycerol solution for further analyses.

4.4 Measuring Enzyme Concentration

A modified Lowry method (Bio-Rad Dc Protein concentration determination kit, Hercules, CA, USA) was employed in this project to determine the concentrations of all the purified mutated prolidases. The bovine serum albumin (BSA) solutions were prepared at several known concentrations such as 0.2, 0.4, 0.8, 1.2 and 1.8 mg/mL to determine the standard curve of the Lowry method. The BSA solutions were added in Bio-Rad reagent A and B at a 1: 5: 40 ratio to allow colour-developing reaction for 15 min. The absorbances of the samples were then measured at wavelength of 750 nm using spectrophotometer Beckman Coulter DU800 (Fullerton, CA, USA). The standard curve obtained through fitting BSA concentrations versus absorbances to a straight line. The standard curve was calculated as

$$[E](mg/ml) = 3.968 \times Abs - 0.366 \qquad \text{(Equation 4.1)}$$

The concentrations of studied 11 mutants were all determined using this standard curve of the Lowry method.

4.5 Enzyme Activity Assay

The enzyme activity assay was performed by using a ninhydrin method (Doi et al., 1981). The released amount of free proline was determined by the colour developing reaction between ninhydrin and proline. The ninhydrin solution was formulated as 3g ninhydrin dissolved

in100mL organic solvent (acetic acid: phosphoric acid= 6:4/V: V) and was heated to 70°C to dissolve ninhydrin.   In order to create a standard curve, the known concentration of free proline solutions was reacted with the ninhydrin solution, and it showed a linear relation to the absorbance of the yielded chromophore.   The substrates and free amino acids other than proline did not generate any chromophore under these conditions.

Before conducting enzyme activity assay on each prolidase, the concentration of the purified prolidase to be employed in the assay was determined in order to allow keeping initial reaction rates for more than 5 min.   Upon the concern of practical manipulations, the starting point of measuring was chosen at 2 min after reaction started.

The standard enzyme activity assay was performed by preheating 90 µL reaction mixture (RM: 20 mM sodium citrate buffer of pH 6.5/ 1 mM zinc chloride/ 2 mM Leu-Pro substrate) at 50°C in the waterbath for 2 min.   Then a 10 µL purified enzyme preparation was added to the RM to start the reaction.   The enzyme reaction was kept in the waterbath for the whole time length until the enzyme activity was quenched in the ninhydrin solution.   Two minutes after the start of reaction, 20 µL of the mixture was taken out from the reaction reservoir and then immediately quenched by adding a 100 µL ninhydrin solution.   The sampling procedure was repeated at every minute thereafter and four points were obtained in total until 5 min after the start of reaction.   The samples were heated on heating block at 100°C for 10 min and then immediately cooled down on ice for the colour-developing step.   The absorbance values of the samples were determined by spectrophotometry using DU800 at the wavelength of 515 nm.

The obtained absorbance values were then converted to the amount of free proline in the samples by multiplying a constant of 0.725549 ABS/μmol, which was determined by a standard curve of amounts of proline vs. absorbance values.   The enzyme activity is represented by the released amount of proline per minute.   Each point of enzyme activity was determined by taking average of the triplicate experiments under each condition.   The enzyme activity v (μmol $\cdot$min^{-1}) was divided by the amount of enzyme (mg) participating in the enzymatic reaction to give the specific activity of the enzyme (μmol $\cdot$ min^{-1} $\cdot$ mg^{-1}).

4.6 Substrate Specificity

The investigation of the substrate specificity of each mutant was carried out by measuring its activities towards nine dipeptides and two tripeptides, which were Leu-Pro, Phe-Pro, Val-Pro, Arg-Pro, Lys-Pro, Gly-Pro, Asp-Pro, Glu-Pro, Pro-Pro, Leu-Leu-Pro and Leu-Val-Pro. The reactions were individually conducted under the optimum conditions (pH 6.5 and 50°C) in the presence of zinc ions using 2 mM dipeptide substrate.

4.7 Metallic ion Dependency

The metallic ion dependency was investigated by measuring each mutant's activity towards eleven peptide substrates in the presence of Mn^{2+} instead of Zn^{2+} at the optimum condition (pH 6.5 and 50 °C). The procedure was similar to that in the study of substrate specificity, with the only difference that 1 mM zinc chloride in the RM was replaced by 1 mM manganese chloride.

4.8 pH Dependency

In the study of pH dependency of each mutant, the reactions were conducted using Leu-Pro as the substrate at different pHs at the optimum temperature 50°C with Zn^{2+}. The different pHs in the reactions were achieved by using different buffer systems. Most pHs required for the study (pH 5, 5.5, 6, 6.5, 7, 7.5, 8, 8.5, 9) were made by mixing 20 mM sodium citrate (pH 4.96) and 20 mM sodium borate (pH 9.23) in different ratios. The two extreme pHs 4 and 10 were achieved using 20 mM citrate-HCl buffer and 20 mM sodium borate buffer, respectively. The RM for each mutant was composed of 1 mM zinc chloride, 2 mM dipeptide substrate (Leu-Pro, Asp-Pro or Arg-Pro), and the aforementioned buffer component. The enzyme reactions and the colour-developing reactions were processed in the same manner as the standard enzyme assay. The calculated enzyme activities at various pHs were transformed to relative activities to the enzyme activity at pH 6.5 (for Leu-Pro) and pH 7.0 (for Asp-Pro and Arg-Pro) for the construction of the pH dependency profile of each mutant.

4.9 Thermal Dependency

The RMs for each mutant's reactions at different temperatures were the same as that in the standard enzyme assay (20 mM sodium citrate buffer of pH 6.5/ 1 mM zinc chloride/ 2 mM Leu-Pro substrate solution).   Temperatures employed were 20, 30, 35, 40, 45, 50, 55, 60, 70, and 80 °C for the study of the thermal dependency of enzyme activity.   Temperature was controlled constantly in a waterbath.   The enzyme activities were plotted against temperatures to show the thermal dependency profile of each mutant.

4.10 Kinetics Study

Each of the purified mutated prolidases was analyzed by the kinetics study with the expectation of interpreting the allosteric behaviour and substrate inhibition of the *L. lactis* Prolidase.   The reactions were performed under different concentrations of Leu-Pro at the optimum condition (pH 6.5, 50°C with zinc ions).   The used substrate concentrations were 0.1, 0.2, 0.3, 0.4, 0.5, 0.7, 1, 2, 4, and 8 mM.   The RMs were 20 mM sodium citrate buffer of pH 6.5, 1 mM zinc chloride and Leu-Pro at a target concentration.

Then the reactions were operated in the same procedure of the standard enzyme activity assay.   Michaelis constants and V_{max} values were determined initially with the data from the substrate concentration range where obvious substrate inhibition was not observed.   This preliminary V_{max} was used to calculate the preliminary Hill constants as the slopes of linear regression of Ln $[v/ (V_{max}-v)]$-Ln S plot.   These preliminary numbers were used as the starting values for direct fitting of the data to Equation 4.2 using the Profitcurve-fitting software (Quantumsoft, Uetikon am See, Switzerland, http://www.quansoft.com/).   The kinetic parameters determined include the maximum velocity (V_{max}), the affinity constant ($K_{0.5}$), the Hill constant (h) and the substrate inhibition constant (K_i).

$$v = \frac{V \cdot s^h}{K_m + s^h + \dfrac{K_m \cdot s^{2h}}{K_i}} \qquad \text{(Equation 4.2)}$$

4.11 Statistical Analyses

Different statistical methods were chosen and applied on the studies of substrate specificity, pH and thermal dependency of enzymes, and the model assumptions were evaluated to determine whether the model fitting was appropriate and the derived results were useful.

In the study of substrate specificity, the nested ANOVA model was chosen by considering enzyme activity ("*act*") as the single continuous response variable, "*substrate*" as one categorical explanatory variable and the factor of "*enzyme*" nested in *substrate*. The nested ANOVA model was then constructed by applying the *lm* function with the model formula of *act~substrate/ enzyme* (Crawley, 2007). The constructed model was translated as *act* responding to different levels of *enzyme* nested in *substrate*. The *p*-value in this model was smaller than 2.2e-16, indicating that the differences of the means of *act* among *enzyme* (nested in *substrate*) were significant at 0.1%. This model was then plotted to check the assumptions of the ANOVA model (see Appendix A).

In the study of pH dependency, the statistical analysis was first conducted on the relationship of activity to the pH change in each research object (referring to each enzyme in the presence of different substrates), such as the pH dependency profile of wild type prolidase towards substrate Leu-Pro. The enzyme activity was considered as the continuous response variable, and the pH value was the continuous explanatory variable. The scatter plot of all data points in every object revealed a non-linear relationship between enzyme activity and pH, and there was no theoretical equation describing the shape of such relationship. For these reasons, generalized additive models (GAM) were chosen for the non-linear regression of enzyme activity versus pH by using non-parametric smoothers (Crawley, 2007). The formula used to specify the GAM model was simply expressed as *act ~ s* (*pH*) using the non-parametric smoother function "*s*". Then the slopes of activity change in this pH range were calculated by predictions from the established GAM model of each object. In the biological meanings, these slopes indicated the extent that the enzyme activity was influenced by the pH change. By comparisons of the slopes of a certain enzyme with charged substrate Asp-Pro or Arg-Pro to its slopes when using a neutral substrate

Leu-Pro, it could be stated whether the substrate specificity was related to the electrostatic nature of the S_1 substrate binding subsite and which residue had the most effect on this character. The one-way ANOVA was used with the slopes of activity change in the range of pH 0.5 increment between pH 5 and 7 as single continuous response variable and research object (enzymes with different substrates) to be the categorical explanatory variable. The non-linear regression and one-way ANOVA were carried on by utilizing the functions of *gam* and *lm*, respectively, in the R software (Crawley, 2007). And the results of models following the assumptions were plotted to check their applicability for the study of pH dependency (see Appendix A).

4.12 Molecular Modelling

Using the NAMD2 molecular modeling program (Kal *et al.*, 1999), the molecular models of the nine mutants were created with an energy-minimizing calculation based on the molecular model of wild type prolidase (Yang & Tanaka, 2008). The wild type model was generated with 3D-JIGSAW server based on the crystallographic model of *Pyrococcus furiosus* OT3 (PDB 1PV9). Initial models of each mutant prolidase were created by substituting target amino acids on SWISS-PDB Viewer (Kaplan & Littlejohn, 2001). The initial models were then subjected to the energy-minimization calculation using the NAMD2 program. The calculation was carried out in a water-filled box using the topology force field data provided with the program. The cut-off distance was set to 15 Å and the calculation was run 5000 times. The energy-minimizing models were then subjected to the VMD molecular visualizing program (Humphrey *et al.*, 1996) to analyze the relations of the substituted residues in the active site.

5 RESULTS and DISCUSSIONS

5.1 Mutations of pepQ Gene

The DNA sequencing results of all single and combined mutants were validated to be the correct nucleic acid sequences using the BLAST database in the PubMed online services. Results showed that recombinant *E.coli* cells containing all mutated prolidases have been successfully constructed with designed mutations.   An example of the nucleic acid sequence of one mutant is depicted in Figure 5.1-1.

5.2 Purification of Mutated Prolidases

All mutated prolidases were purified by four sequential steps: crude extraction, ammonium sulfate precipitation, DEAE-Sephacel and Phenyl Sepharose chromoatography.   The samples were examined on SDS-PAGE after every purification step to confirm and identify the existence of prolidase.   Since all the prolidases were purified under the same conditions and had the same behaviour in the purification steps, the obtained prolidases should be properly folded to have catalytic activities.   The protein concentrations and enzyme activities were also measured after each purification step (Table 5.2-1).   The activity of each sample was measured using 2 mM Leu-Pro as substrate at pH 6.5 and 50°C, following the procedure of the standard enzyme assay as stated in the section of Material and Methods.

The purification of L193R mutant prolidase is taken as an example.   A 300-mL culture yielded 5 mg of the purified L193R enzyme, with a purification fold of 7.8.   The total activity after each treatment decreased by nearly a half of the activity before that, and 12.2% of the total activity was recovered from the crude extract.   However, to optimize the purification process of the mutated prolidases was not a necessity for this project.   The obtained amounts of purified mutated prolidases were sufficient for the characterization experiments to interpret the

```
GGA TGATCA CGA ……ACA CGGAAG TAC TAT CAG L193E/V302D mutant

GGA CGTTCA CGA ……ACA CGCTTG TTT TAT CAG Wild type
```

Figure 5.1-1 The comparison of the segments.

Segments of nucleic acid sequence of the pKK223-3 mutant with combined mutations

of V302D and L193E compared with the corresponding segment in the wild type.

Table 5.2-1 The purification of the mutant L193R.

Purification process	Total protein (mg)	Specific activity (μmol·min^{-1}·mg^{-1})	Yield (% activity)	Purification (fold)
Crude extract	318.9	9.0	100	1
Ammonium sulfate precipitation	108.8	15.8	59.8	1.8
DEAE-Sephacel chromatography	17.8	45.9	28.4	5.1
Phenyl Sepharose chromatography	5.0	70.6	12.2	7.8

structure-function relationship of the prolidase at the S_1 site.

5.3 Characterization of Mutated Prolidases

5.3.1 Substrate Specificity

The activities of each mutant to different substrates were measured under the optimum conditions of wild type prolidase (Yang & Tanaka, 2008). The relative activities to different substrates of each mutant were displayed as percentages to the activity using Leu-Pro as the substrate (Table 5.3-1). All the Phe190 mutants lost their activities to any substrate, thus omitted from Table 5.3-1. The Leu193 and Val302 mutants retained activities, and exhibited various substrate specificity profiles, which are presented by different relative activities to eleven substrates including dipeptides (Leu-Pro, Asp-Pro, Glu-Pro, Arg-Pro, Lys-Pro, Phe-Pro, Val-Pro, Pro-Pro and Gly-Pro) and tripeptides (Leu-Leu-Pro and Leu-Val-Pro) (Table 5.3-1).

The statistical analyses interpreted the observations of mutants' substrate specificities in more details, based on the data obtained from Table 5.3-1. Table 5.3-2 listed the statistically calculated differences of each mutant's activity from the corresponsive activity values of the wild type for each substrate (for statistical analyses please refer to Appendix B).

Table 5.3-2 shows the differences in the substrate specificities between the wild type and mutant. Larger values marked with three asterisks mean the mutant preferred the particular substrate more than the wild type. Compared with wild type prolidase, the L193T mutant exhibited preferences towards Lys-Pro, Arg-Pro and Phe-Pro, and the mutant V302T took more Lys-Pro and Arg-Pro. The substrate specificity profile of the V302K mutant was almost the same as that of wild type prolidase. Both V302D and L193E mutants showed more preferences to Lys-Pro and Arg-Pro. The V302D and L193R mutants had evident activities to the anionic Asp-Pro that the wild type did not hydrolyze at all. Since the V302D mutant took both positive and negative dipeptides as substrates, it would be interesting to see how the activities changed to Lys-Pro and Arg-Pro in the L193E/V302D mutant or to Asp-Pro in the L193R/V302D mutant. Results showed that a double mutant L193R/V302D had activity to Asp-Pro similar to each single mutant of L193R and V302D. However, the other double mutant L193E/V302D did not

Table 5.3-1 Relative activities to different substrates in the wild type and mutated prolidases.

	Relative activity (%) (Leu-Pro=100%)								
	Wild type	L193E	L193R	L193T	V302D	V302K	V302T	L193R/V302D	L193E/V302D
	(468.7±6.6)	(99.6±5.2)	(118.8±10.6)	(67.3±2.5)	(14.1±1.6)	(55.9±7.7)	(73.5±1.7)	(7.5±0.6)	(0.95±0.1)
Leu-Pro	100±1.4	100±5.9	100±8.2	100±2.5	100±5.6	100±0.9	100±4.2	100±5.6	100±4.8
Asp-Pro	N.D.	5.9±0	37.0±9.0	N.D.	25.9±1.6	2.6±0.5	3.4±1.6	33.0±2.6	16.0±0.9
Glu-Pro	N.D.	2.0±0.3	2.5±0.7	11.4±2.5	7.4±3.2	N.D.	2.0±1.0	24.9±1.3	20.0±1.8
Arg-Pro	12.0±0.9	51.0±9.0	1.9±1.0	81.4±4.3	57.4±5.6	5.7±0.9	32.8±2.1	13.8±0	62.0±5.6
Lys-Pro	6.6±0.5	39.2±6.8	2.3±0.3	48.6±10.8	31.5±1.5	4.1±0.9	37.5±1.8	19.2±2.8	78.0±8.3
Phe-Pro	23.8±0.4	33.3±6.8	20.2±2.9	278.6±8.6	59.3±6.4	8.8±2.9	14.5±0.6	21.9±3.4	180.0±16.5
Val-Pro	14.4±0.4	70.6±0	11.1±1.4	34.3±4.3	N.D.	29.4±0	46.0±3.1	2.7±0.6	N.D.
Pro-Pro	N.D.	3.9±0.6	0.7±0.3	14.3±1.2	7.4±3.2	N.D.	N.D.	N.D.	N.D.
Gly-Pro	N.D.	N.D.	2.9±0.9	2.9±0.9	N.D.	N.D.	1.0±0.2	N.D.	N.D.
Leu-Leu-Pro	N.D.	3.9±0.7	N.D.	N.D.	N.D.	N.D.	N.D.	N.D.	N.D.
Leu-Val-Pro	N.D.	9.8±1.4	N.D.	N.D.	N.D.	N.D.	N.D.	N.D.	N.D.

N.D. refers to "not detectable".

Data in parentheses refer to specific activities (μmol/min·mg) of prolidases using 2 mM Leu-Pro as substrates.

Table 5.3-2 The differences in substrate specificities of mutants compared with the wild type [a].

Substrate/Charge		L193E	L193R	L193T	V302D	V302K	V302T	L193R/V302D	L193E/V302D
Leu-Pro	neutral	-5.56	-7.73	-2.78	-5.26	-0.51	-3.27	-3.64	-1.96
Asp-Pro	negative	5.56	34.13***	2.78	24.56***	2.56	3.27	31.77***	15.68
Glu-Pro		1.85	2.27	11.11	7.02	2.4E-15	1.96	23.96***	19.61**
Lys-Pro	positive	30.43***	-4.47	40.62***	23.23***	-2.49	29.67***	11.89	69.87***
Arg-Pro		36.15***	-10.27	67.17***	42.39***	-6.36	19.7**	1.28	48.78***
Val-Pro		52.27***	-4.13	18.93**	-10.89	14.83**	30.02***	-11.80	-10.48
Gly-Pro	neutral	9.97E-16	2.67	2.78	3.51	0.51	0.98	0.78	9.80
Pro-Pro		3.7	0.67	13.89	7.02	1.03	0	1.60	6.25

a: Mean of each mutant's activity (%) to a certain substrate － mean of wild type prolidase's activity (%) to the same substrate

*** $P<0.001$, meaning most significant differences from wild type prolidase

**$P<0.01$, meaning relatively significant differences from wild type prolidase

show significant changes in activity to Asp-Pro while it had increased preferences to cationic substrates Lys-Pro and Arg-Pro and a hydrophobic substrate Phe-Pro.   L193R/V302D had activity to Asp-Pro similar to each single mutant of L193R and V302D.   However, the other double mutant L193E/V302D did not show significant changes in activity to Asp-Pro, while it had increased preferences to cationic substrates Lys-Pro and Arg-Pro, and a hydrophobic substrate Phe-Pro.

To interpret these observations, the molecular modelling was conducted to investigate the conformational changes of the S_1 site and neighbouring residues in each mutant.   The models of the active sites of the single mutants and double mutants were generated using the NAMD2 and VMD molecular visualizing software (Figure 5.3-1).

The Phe190 mutants did not have significant activities to Leu-Pro dipeptide.   In the model of F190E (Figure 5.3-1), a relocation of one catalytic zinc ion was observed at a large degree. Negative charged Glu190 coordinated one of the zinc ions, causing the disruption of its original coordination with Glu339, which was coordinated with both zinc ions in wild type prolidase. The loss of activity and the molecular models suggested that Phe190 was an important residue to keep the zinc positioning, the structure of the S_1 site, and thus the catalytic activity of prolidase.

The observed activities of mutants at position 193 were concluded to follow the assumption that the introductions of charged functional groups at the S_1 site would influence the electronic nature of preferred substrates.   At pH 6.5 (the standard condition used for all the enzyme assays in the study of substrate specificity), the activity of L193E mutant was increased towards the cationic substrates Lys-Pro and Arg-Pro due to the negative charge introduced at S_1 site via the deprotonation of Glu193.   In contrasts, the Arg193 in L193R would have positive charge by the protonation at that pH, thus to take anionic dipeptide Asp-Pro as the substrate.

Whereas the Leu193 mutants hydrolyzed the dipeptides with opposite charges, a position-302 mutant (V302D) was able to catalyze both anionic and cationic substrates disobeying the assumption.   The substituted residue Asp302 should be deprotonated and should have a negative charge at pH 6.5.   The positively charged substrates like Lys-Pro and Arg-Pro

(a)

(b)

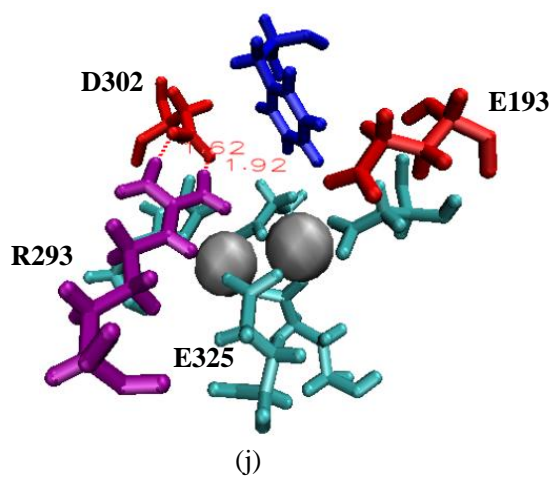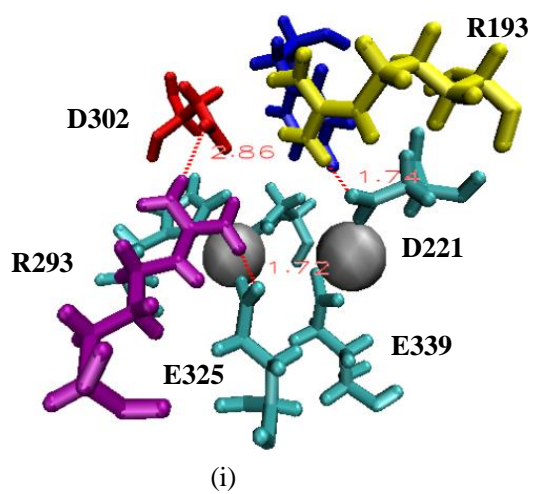(c)

(d)

(e)

(f)

(g)

(h)

(i)

(j)
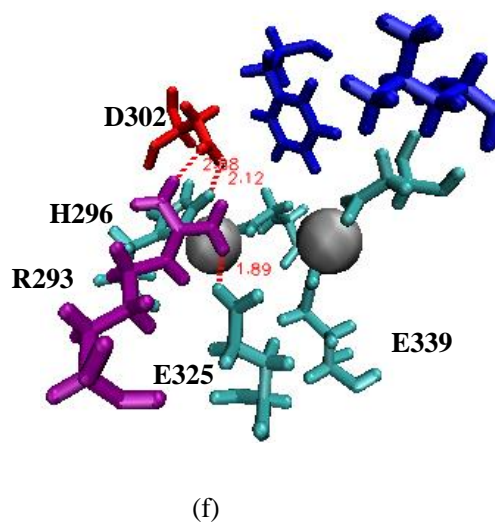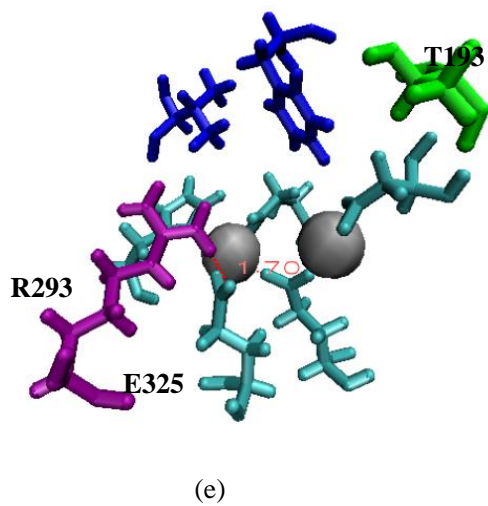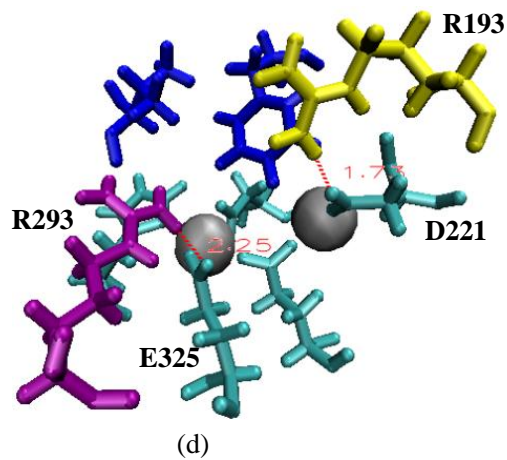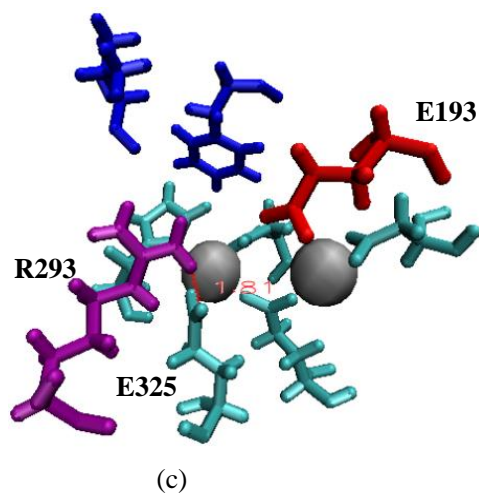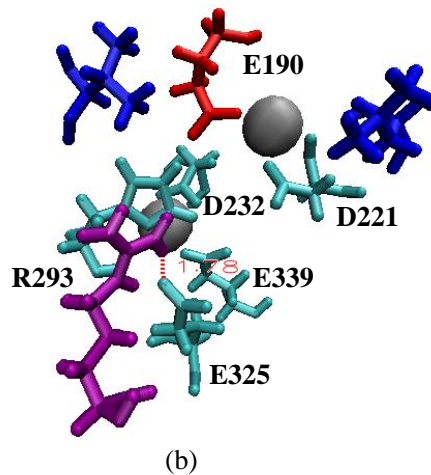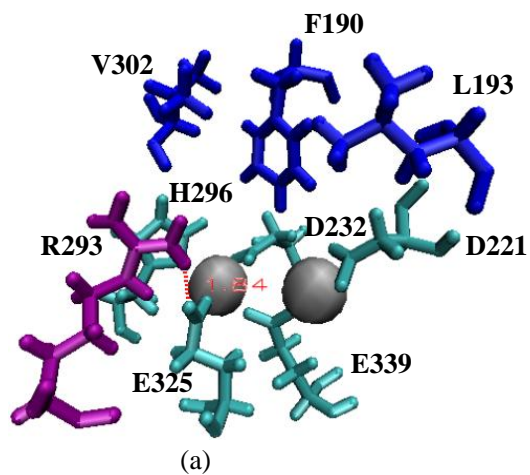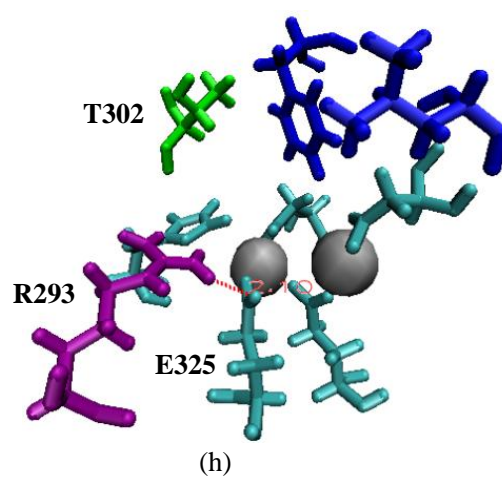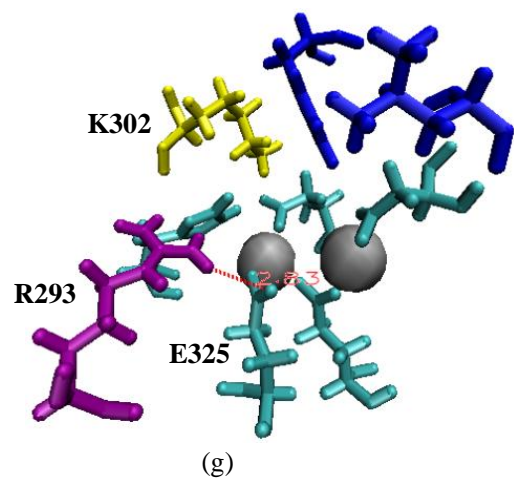
Figure 5.3-1 The illustrations of molecular modelling of the single mutants and wild type prolidase.

Each model shows (a): wild type prolidase; (b): F190E; (c): L193E; (d): L193R; (e): L193T; (f): V302D; (g): V302K; (h): V302T; (i): L193R/V302D; (j): L193E/V302D.   All residues are shown in licorice models, and zinc ions are grey balls.   The S_1 site (Leu193, Phe190 and Val302) of wild type prolidase is represented in blue.   The mutated residues are differentiated by colours according to their electronic nature.   Negative and positive charged residues at the S_1 site are red and yellow, respectively, and polar residues are in green.   The cyan licorice models are metal-chelating residues (Asp221, Asp232, His296, Glu325 and Glu339).   The purple licorice model represents the key residue Arg293 to the allosteric behaviour.   Some bonds are displayed with values of distances (Å) in the models of the wild type and mutated prolidases.

would be accommodated by Asp302 to bind selectively in the S_1 site, resulting in a higher rate of hydrolysis.   It was interesting that V302D also showed activity to negatively charged substrate Asp-Pro, which was expected to be excluded from the S_1 site of the V302D mutant.   This contradictory result could be explained as the effects of its neighbouring residues.   According to the molecular model of V302D (Figure 5.3-1 (f)), the mutated residue Asp302 flanked positively charged residues His296 and Arg293.   Compared to wild type prolidase, the opposite-charge attractions would keep His296 and Arg293 close to Asp302, by distances of 2.12 and 2.88 Å, respectively.   Therefore His296 and/or Arg293 would stabilize Asp302 at the S_1 site via opposite-charge attraction, and consequently formed a hydrophilic environment for the anionic substrate.   Although V302D could hydrolyze substrates with both charges, this mutant showed lower catalytic efficiency (V_{max}/ K_m) compared to the L193E mutant (Section 5.3.3, Table 5.3-5). The lower catalytic efficiency of V302D suggested that the mutations at position 302 could have larger influence on the active centre than that at position 193.   In metal peptidases, a residue acts as the proton acceptor to allow a water molecule to form the catalytic intermediate with the peptide substrate.   The results of pH dependency suggested that the catalytic residue (*i.e.*, proton acceptor) had a pK_a value of approximately pH 5 to 6.   Since free histidine has a pK_a at pH 6.0, His296 likely worked as the catalytic residue to accept a proton from the water attacking the amide bond of the substrate for the hydrolysis.   At neutral pH, His296 can accept a proton, but His296 would not accept any proton once it is protonated at acidic pH.   The introduction of a polar (charged) residue in the S_1 site would affect the hydrogen bond network, resulting in an altered protonation tendency of this histidine.   The observations suggest that mutations at position 302 affected the electronic state of the nearby His296, thus to influence the prolidases activities.

The substrate specificity of V302K was observed similar to that of the wild type, showing the highest activity to hydrophobic Leu-Pro dipeptide and no significant activity to polar substrates.   This observation indicated that the substitution of valine at position-302 by cationic lysine did not affect the substrate specificity of prolidase.   As illustrated in the molecular model

of V302K (Figure 5.3-1 (g)), Lys302 was located closely to the positive residues Arg293 and His296. Lys302 would be possibly in the neutral form through effects of neighbouring residues with the same charge as discussed in the part of literature survey (section 2.5). Thus the S_1 substrate binding subsite would be maintained in the neutral state to accept hydrophobic substrates.

The combined mutant L193R/V302D increased in the activity to Asp-Pro, but a little activity changes was shown in the combined mutant L193E/V302D. The combined mutant L193E/V302D exhibited relatively higher preferences to the cationic substrates Lys-Pro and Arg-Pro, while these dipeptides were poor substrates for the combined mutant L193R/V302D compared with the single mutant V302D. Considering the V302D mutant hydrolyze both cationic and anionic dipeptides, these observations indicated that the mutation at position 193 had more effect on the preferences towards charged substrates than that at position 302. In other words, the residue Leu193 was the determining residue for the substrate specificities to hydrophobic dipeptides in wild type prolidase. The mutation L193R maintained relatively high catalytic efficiency (V_{max}/ K_m) than the other mutants as discussed later (Section 5.3.3, Table 5.3-5). Also in the molecular modelling, the conformational changes in the L193R did not significantly affect the positions of the two catalytic zinc ions at the S_1 site. It was concluded that the mutation of L193R expanded the substrate specificity to the anionic peptide Asp-Pro without disrupting the three-dimensional structure of the active site.

In conclusion, the charged substitutions of the S_1 site residues did affect the polarity of the S_1 site, making mutated prolidases present different specificities towards charged substrates. The mutations on residue Leu193 of the wild type showed expected changes of substrate specificity according to the charge of substitutions. In contrast, rather than the direct influences of residues at position 193 on the charges of the substrate binding site, the Val302 mutations presented effects on the prolidases activities via interactions with His296, which was proposed to be a proton acceptor in the nucleophilic attack of prolidases. Therefore, Leu193 was suggested to have more effect than Val302 did on substrate specificities of prolidases.

5.3.2 pH Dependency

The pH dependency profiles of wild type and mutated prolidases are presented as curves of relative activities versus different pH values (Figure 5.3-2). The activities of each prolidase were measured using Leu-Pro dipeptide as the substrate at the optimum temperature, 50°C, over a range of pH from 4.0 to 10.0. The activities of some prolidases in the presence of charged dipeptide substrates were also investigated and compared with those to Leu-Pro (Figure 5.3-2): they were activities of L193E, V302D and wild type prolidases to cationic dipeptide Arg-Pro; and those of V302D and L193R to anionic dipeptide Asp-Pro.

All eight active mutants obtained in this study and wild type prolidase showed bell-shaped profiles of pH dependency to different substrates. Wild type prolidase catalyzed the reaction in a range of pH 6.0 to 8.0 with highest activity at pH 6.5 (Yang & Tanaka, 2008). Compared to the wild type, all mutated prolidases exhibited activities to substrates in a broader pH range of 5.0 to 8.0 with the optimum pH at 6.0 or 6.5. It was interesting to notice that the mutants maintained relatively higher activities at extreme pH of 5.0 and 8.0. For example, the mutants L193E, L193T, V302D and V302T had activities around 50% relative activities at pH 5.0, and all six single mutants at position 193 and 302 exhibited much higher activities (from 68.1% to 90.0%) than the wild type at pH 8.0.

The relationships of relative activities and pH values in prolidases were expressed statistically into coplots (see Appendix B). The slopes of the regression curves were calculated for each 0.5 increment out of these coplots (Table 5.3-3), and were used to compare the effects of pH changes among enzymes and substrates to investigate the assumption that the interactions between substituted residue at the S_1 site and charged side chains in the substrates would influence the mutant's substrate specificity. These influences were perceived in two different ways: the different profiles of pH dependency in various mutated prolidases were observed to the same substrate, leading to the research of the influence from substituted residues at the S_1 site; In a certain pH range, the mutated prolidases showed activities' decreases in different extents towards different substrates, indicating the joint influence of mutated S_1 residues and

a

b

c

d

e

f

52

g

h

53
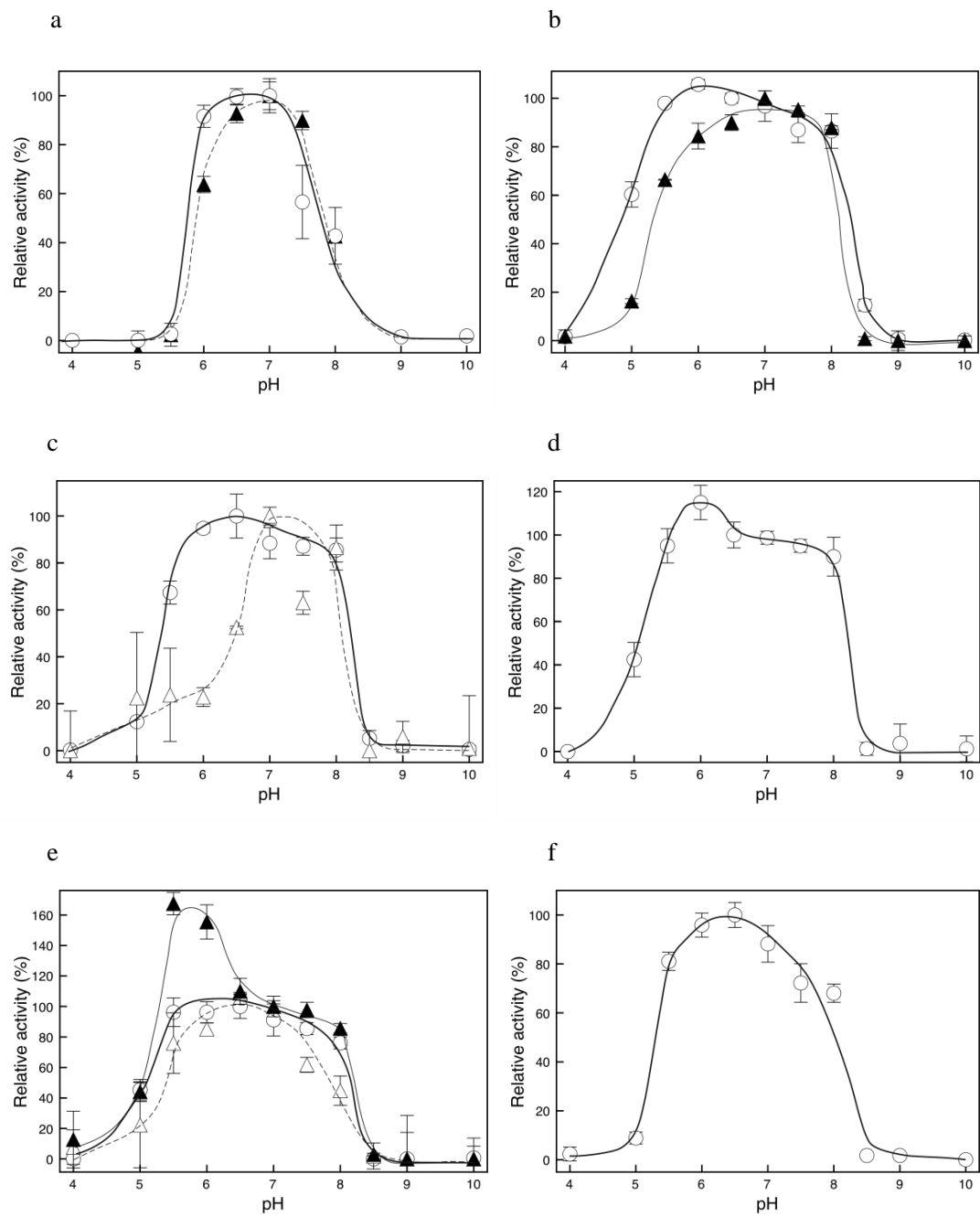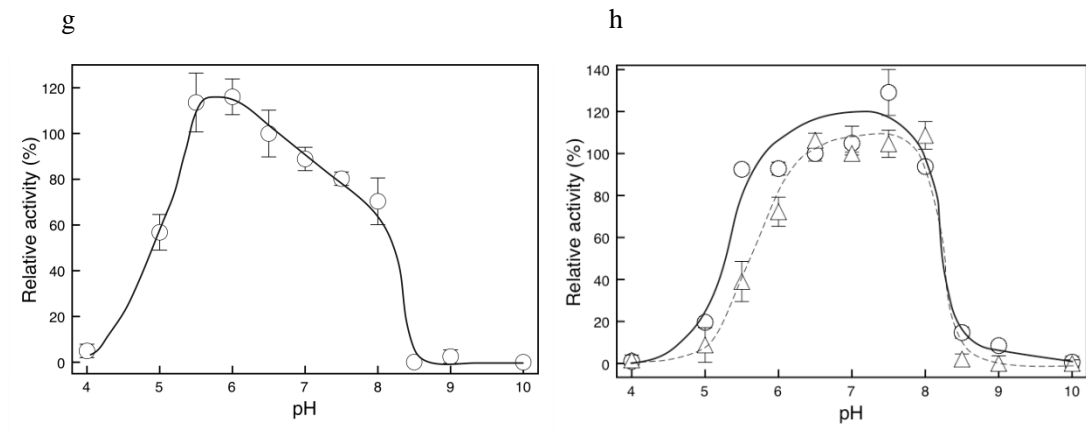
Figure 5.3-2 pH dependency of each enzyme's activity to Leu-Pro.

The observed activity at each pH was plotted as relative activity to the activity at pH 7 for Leu-Pro and at pH 6.5 for Asp-Pro and Arg-Pro. Thick solid lines and open circles (—○—) indicate dependency with Leu-Pro as the substrate, dotted lines and open triangles (----△----) present dependency with Asp-Pro, and thin solid lines and solid triangles (—▲—) present dependency with Arg-Pro. Error bars indicate the standard error values for triplication. a) Wild type, b) L193E, c) L193R, d) L193T, e) V302D, f) V302K, g) V302T, h) L193R/V302D

Table 5.3-3 Differences of enzymes' pH dependences in the range of pH 5.0~5.5, 5~5.5, 5.5~6.0, 6.5~7.0.

Enzymes /Substrate	Means of slopes in the range of			
	pH 5.0 ~ 5.5	pH 5.5 ~ 6.0	pH 6.0 ~ 6.5	pH 6.5 ~ 7.0
WT/Leu-Pro	31.39	143.76***	13.32	20.87
L193E/Leu-Pro	80.44***	31.45	10.68	-14.27
L193R/Leu-Pro	121.98***	48.64**	24.59	-40.01**
L193T/Leu-Pro	116.17***	40.96**	21.52	-9.66
V302D/Leu-Pro	110.34***	37.99	17.99	-12.78
V302K/Leu-Pro	154.00***	44.62**	31.43	-1.88
V302T/Leu-Pro	126.53***	28.53	-0.02	-27.94
WT/Arg-Pro	14.73	124.25***	59.95**	15.30
L193E/Arg-Pro	122.38***	24.59	35.64	-3.77
L193R/Asp-Pro	18.18	38.75	47.80**	27.47
V302D/Asp-Pro	91.54***	16.79	41.53**	-18.06
V302D/Arg-Pro	247.05***	25.53	-8.21	-34.91

[a] represented by the differences in the mean value of slopes of the non-linear regression curves of enzyme activities versus pHs in the range of pH 5~5.5. E.g. the value at the first left top is calculated as: -86.79 = mean value of slopes from the wild type － mean value of slopes from L193T.

Significant codes: *** $P < 0.001$, ** $P < 0.01$, *$P < 0.1$.

charged side chains in the substrates.

Based on the data in Table 5.3-3, some overall observations can be made that 1) wild type prolidase had a drastic activity drop between pH 5.5~6.0 towards Leu-Pro or Arg-Pro; 2) the activities of most mutated prolidases to various substrates had largest drops in the range of pH 5.0~5.5; and 3) L193R was an exception among mutants by showing activity drop to anionic substrate Asp-Pro in the range of pH 6.0~6.5.

Since the significant activity decreases of the mutated prolidases all happened in the range of pH 5.0~5.5, further statistical analyses were conducted to study how these decreases related to the different mutations and substrates within this pH range. The results (included in Table 5.3-3) were derived from the boxplots in these analyses (details of statistical analyses described in Appendix B). The statistical analyses showed that the activity of L193E to cationic substrate Arg-Pro steeply decreased in the pH range of 5.0~5.5 more than that to Leu-Pro.   The difference of the slope between Asp-Pro and Leu-Pro reached 41.94.   The L193R mutant had a much less activity change from pH 5.5 to pH 5.0 with Asp-Pro compared to its activity change to Leu-Pro. The V302D mutant exhibited the largest decrease in activity to Arg-Pro from pH 5.5 to pH 5.0 in the comparisons of its activity decreases when using other substrates.

In the molecular model of the wild type (Figure 5.3-1), five residues (His296, Asp232, Asp221, Glu325 and Glu339) were observed to be the metal-chelating residues which had direct bonding with the catalytic zinc ions. Among them, His296 was proposed in Section 5.3.1 to have coordination with the zinc-bound water molecule and to act as a general base in the deprotonation of the water molecule for the nucleophilic attack. Histidine residue can be protonated, but its pK_a value is much lower than other two cationic amino acids, arginine and lysine (Table 5.3-4).   This pK_a of histidine suggested that acidification might protonate His296 in the pH range of 5.5~6.0, losing the capacity of accepting a proton from the nucleophile water molecule and thus leading to the activity loss of wild type prolidase.

To maintain the prolidase's activity at lower pH than the value of 6.0, His296 should somehow remain in the deprotonated form below pH 6.   Judging from the molecular modelling,

Table 5.3-4 pK_a values of their side chains.

Amino acids	Conjugate acid	pK_a
Arginine	Guanidinium-NH_2^+	12.48
Histidine	Imidazole-NH^+	6.0
Aspartic acid	β-COOH	3.86
Glutamic acid	γ-COOH	4.25
Lysine	ε-NH_3^+	10.53

the positive charge of Arg293 could interact with His296 because of their close locations. And the introduced residue at positions 193 and 302 could affect the interaction between Arg293 and His296, resulting in the change of pK_a of His296. The following discussions will focus on individual changes of the protonation form of His296 which were only determined by the mutations at the S_1 site without considering the influences from substrates.

The substitutions of Val302 would directly influence the electronic environment around His296 due to its close location to His296 (Figure 5.3-1). In the V302K mutant, the substituted Lys302 with positive charge could prevent the protonation of His296 at pH 5.5, according to the theory that the positively charged group will lower the pK_a of the neighbouring positively charged group, facilitating deprotonation of that group to avoid the like-charge repulsion (Harris & Turner, 2002). Then the stabilized deprotonated form of His296 could keep receiving the proton from the metal-bound water molecule to facilitate nucleophilic attack at pH 5.5, leading to higher activity under more acidic conditions compared to wild type prolidase. The V302D mutation, which brought in negative charge to the S_1 site, also had more tolerance to the acidic condition than the wild type, though its activity was observed to have a larger decrease than that of V302K from pH 5.5 to pH 5.0. This observation might be explained in a way that the anionic Asp302 brought Arg293 and His296 closer to each other in the V302D mutant, to keep the deprotonated form of His296 based on Harris and Turner's theory.

The mutations at the position 193 also exhibited more acidic tolerance than wild type prolidase. The L193R mutation introduced positive charge to the active site, where His296 would tend to retain the deprotonated form at lower pH compared to the wild type to avoid the like-charge repulsion from arginine residues with strong positive charge at positions 193 and 293. The opposite mutation of L193E also had extended working pH range with lower activity at pH 5.5 compared to that of L193R. This observation suggested that negatively charged Glu193 in the L193E mutant influenced His296 by attracting opposite-charged Arg293 towards the catalytic zinc centre, thus towards His296, which coordinated with the catalytic zinc ion. The force that kept His296 in the deprotonated form came from the more closely located Arg293 in the L193E
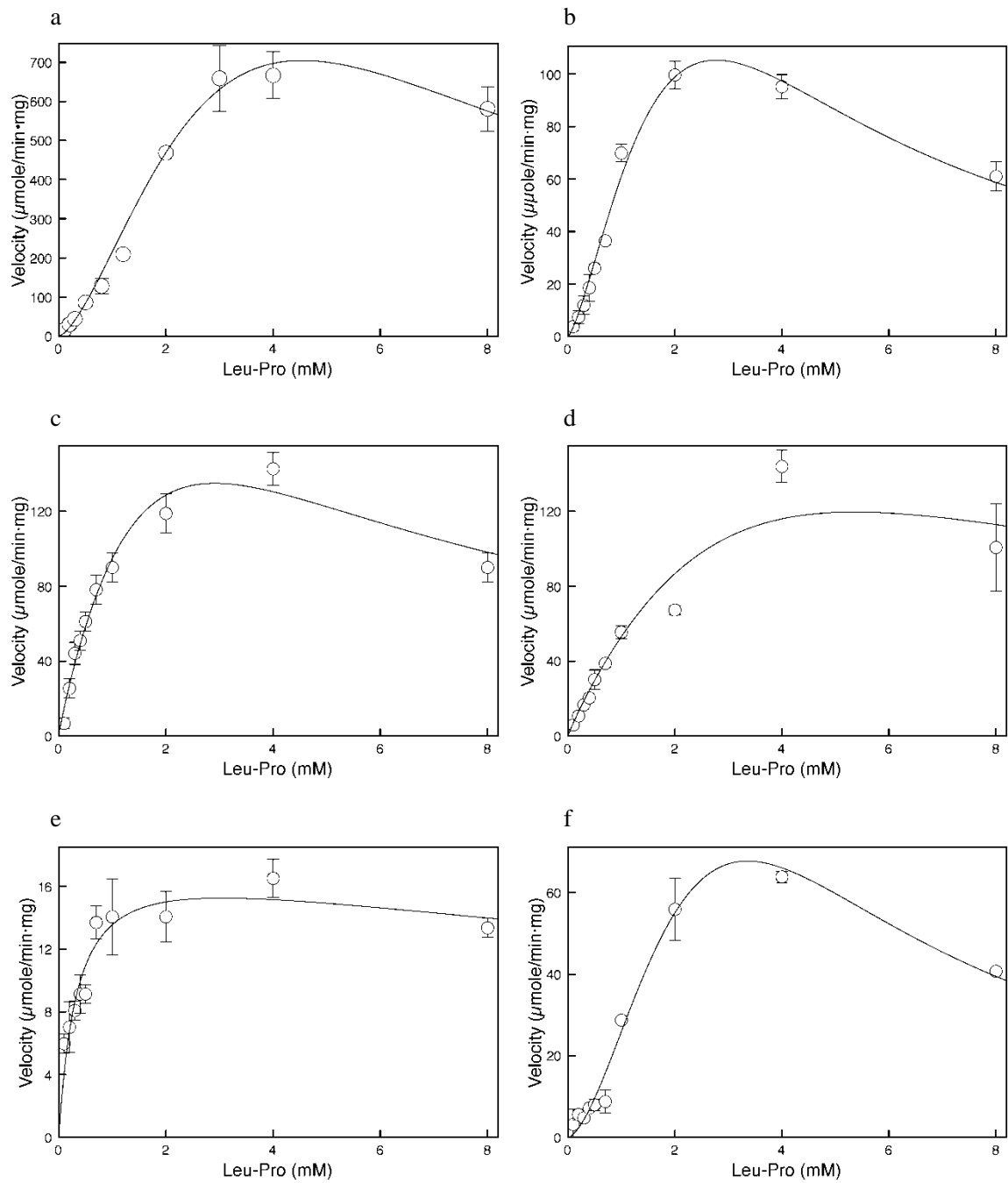
mutant.

When further perceiving the influences on His296 by both the mutations and side chains of substrates, it was proposed that the mutant would have higher activity at certain acidic pH to any positively charged substrate and have lower activity in the presence of anionic substrates. The results from the comparison of mutants' activities to differently charged substrates were in accordance to the deduction: L193E and V302D exhibited the preference of cationic Arg-Pro to Leu-Pro at pH 5.5; L193R and V302D both had decreased activities towards negatively charged substrate Asp-Pro than to Leu-Pro. Moreover, the V302D mutant showed distinguishing higher activity at pH 5.5 when binding to the positively charged substrate Arg-Pro. This observation demonstrated that the binding of charged side chains of substrates at position-302 imposed more effects than that at position-193 on the electronic states of His296 because of the close location of position-302 to -296.

By comparing the differences of pH dependences of mutants to various substrates, it was concluded that the prolidases' activities were indeed affected by the introduced electronic charges to the active site and the charged side chains of substrates. Since His296 was proposed to be involved in the catalytic properties providing a proton to the metal-bound water molecule, it was possible that electronic charges introduced by the mutated S_1 residues and the charged side chains of substrates caused the extended pH ranges of the mutated prolidases' activities via influencing the electronic states of His296.

5.3.3 Kinetics Studies

5.3.3.1 Allosteric behaviour

The relations of substrate concentration and observed catalytic rates were shown in Figure 5.3-3. Since *L. lactis* prolidase shows both allosteric behaviour and substrate inhibition, the equations 2.1 and 2.3 are combined to give Equation 4.2 that describes the allosteric behaviour and substrate inhibition (Equation 4.2) (Parkin, 2003). Then the kinetic constants were determined by fitting the *v-S* plots into this equation.
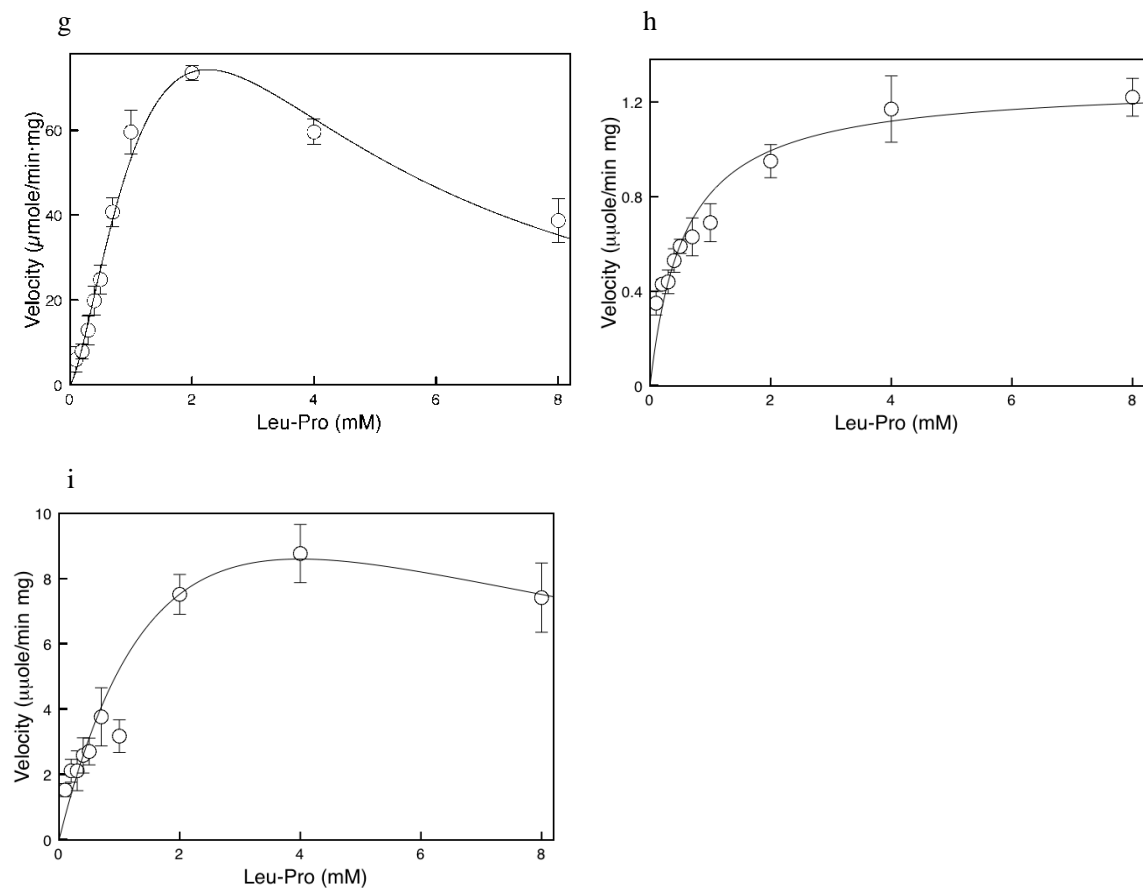
Figure 5.3-3 The *v-S* plots of eight mutants

The lines show the relation between rates and Leu-Pro substrate concentrations (Equation 5.1) with the calculated constants.   a) Wild type, b) L193E, c) L193R, d) L193T, e) V302D, f) V302K, g) V302T, h) L193E/V302D, i) L193R/V302D.

The velocity is expressed as the specific activity in the unit of μmol/min·mg. The kinetic parameters, the maximum velocity (V_{max}), the Hill constant (h), the dissociation constant ($K_{0.5}$) and inhibition constant (K_i) are calculated from the fitting and summarized in Table 5.3-5.

The single mutants L193R, L193T, V302D and double mutants L193R/V302D and L193E/V302D had the Hill constants (h) close to 1. According to the descriptions of allosteric behaviour in the literature review section, these mutants lost the allosteric behaviour that was observed in the wild type. The plots of these non-allosteric prolidases were hyperbolic with constant affinities (K_m), following Michaelis-Menten kinetics at low substrate concentrations. The Hill constants of the L193E, V302K and V302T mutants were larger than 1, indicating that they possessed the cooperativity as shown in wild type prolidase. The v-S plot of a mutant with allostery showed depressions at relatively low substrate concentrations and became much steeper after substrate accumulating to certain concentration.

The loop structure (position 33 to 41 with charged residues Asp36, His38, Glu39 and Arg40 in the middle) have been proposed to be responsible to the allosteric behaviour (Yang & Tanaka, 2008). A recent study on deregulation of allosteric behaviour showed that the loopless mutant lost the activity and the mutation of Arg293 by serine eliminated the allosteric behaviour (Zhang et al., 2009). It was proposed that the interactions between the loop structure and residue Arg293 caused the allosteric behaviour. In this research, the kinetic studies indicated that L193R, L193T, V302D, L193R/V302D and L193E/V302D led to the loss of allosteric behaviour. Based on previous conclusions about the allosteric behaviour, these findings implied that residues Leu193 and Val302 might affect the interactions between residue Arg293 and the loop structure.

In the molecular model of V302D (Figure 5.3-1), Asp302 was located close to Arg293 with a length of 2.88 Å, indicating the formation of a possible ionic bonding between Asp302 and Arg293 via the opposite-charge attraction. This attraction restricted the mobility of Arg293 and also dragged Arg293 away from the loop structure. Combined the model observation and the kinetic data, it is concluded that the restriction imposed by Asp302 would not allow the conformation of allostery determining sites (the loop and Arg293) to respond to the binding of

Table 5.3-5 Kinetic parameters of eight mutants and wild type prolidase.

	Kinetic parameters								
Prolidases	Wild type	L193E	L193R	L193T	V302D	V302K	V302T	L193R/V302D	L193E/V302D
V_{max}(μmol/min·mg)	1740.0	305.6	777.1	761.9	18.3	184.8	166.3	20.2	1.3
h	1.49	1.35	0.91	0.93	1.04	1.60	1.39	1.00	1.00
K_m(mM)	7.0	3.8	6.3	12.8	0.32	6.0	1.92	2.7	0.6
K_i(mM)	90.8	15.7	7.0	22.7	10.2	48.2	9.6	15.7	-
V_{max}/K_m	248.6	81.2	122.5	59.5	57.2	30.6	86.5	7.5	2.2

the substrates, resulting in the loss of allosteric behaviour. In addition, a dissociation of coordination between Arg293 and metal-chelating residue Glu325 was observed in its model, and would be another factor affecting the allosteric behaviour. The loss of the allosteric behaviour in the L193R/V302D mutant could also be explained as the restriction of Arg293's mobility by forming an ionic bond with the negative charged residue Asp302. Further investigation of the model of the L193R/V302D mutant (Figure 5.3-1) suggested that the positive charged Arg193 attracts metal-chelating residue Asp221, causing one of the two coordination of Asp221 with the zinc ion to be dissociated. To compensate the missing coordination, the metal-chelating residue Glu339, which coordinates with both zinc ions in the wild type, was disconnected from the zinc on the side of Asp302 to form two coordinations with the other zinc ion near Arg193. This rearrangement disrupted the connection between two catalytic zinc ions and might cause the much lower catalytic efficiency observed in the mutant L193R/V302D than that in the wild type, as compared by their $V_{\max}$/ K_m values (Table 5.3-5).

In the model of the L193E/V302D mutant (Figure 5.3-1), it was observed that the repulsion between negative charged residues Glu193 and Asp221 caused two zinc ions to come closer to each other. Under this movement of zinc ions, another connection via metal-chelating residue Glu325 was formed between two zinc ions, resulting in the disruption of the ionic bond between the allosteric-determining residue Arg293 and the metal-chelating residue Glu325 in the wild type. In consequence, Arg293 formed an ionic bond with Asp302 and had no binding with any metal-chelating residues. Therefore, the mobility of Arg293 was restricted to cause the loss of the allosteric behaviour in the L193E/V302D mutant.

The allosteric behaviour of wild type *L. lactis* prolidase suggested it to be a regulatory enzyme in the nitrogen metabolism. There have been some supports from previous reports: (i) the branched-chain amino acids (BCAA, isoleucine, leucine and valine) served as the nitrogen signals, provoking the binding of the transcriptional regulator CodY to regulatory sites of its target genes, thus to regress the transcriptions of the genes of important proteases in *L. lactis* such as *pepN* and *pepC* (Petranovic et al., 2004); (ii) the dipeptide Leu-Pro decreased the level of

transcriptions of *pepN* and *pepC* (Guedon et al., 2001);   (iii) the CcpA, a key regulatory enzyme in the carbon metabolism, had a direct effect on the transcription of *pepQ* via a *ccpA-pepQ* link in *L. lactis* (Zomer et al., 2007).   From these findings, it can be depicted how the prolidase functions in the regulation of the nitrogen metabolic pathway.   If there is a sudden oversupply of the dipeptide substrate Leu-Pro, the prolidase would have a quick response to the substrate concentration change facilitated by its allosteric behaviour.   Then the excessive Leu-Pro is consumed quickly to release its stress on the transcriptions of proteases genes *pepN* and *pepC*, thus to help retain the normal degradation of oligopeptides.   In the mean time, the product leucine from digestion of Leu-Pro by the prolidase would be accumulated in the cell.   When amount of this BCAA increases to an extent, it would stimulate the regulator CodY to regress the transcriptions of *pepN* and *pepC*, so that further degradation of peptides to gain amino acids is abolished.

5.3.3.2 Substrate inhibition

Decreased activities at high substrate concentrations were observed in most of the mutants, rather than that the activity reaches plateau in the Michaelis-Menten kinetic.   The same observation was reported in the wild type and interpreted as the substrate inhibition (Yang & Tanaka, 2008).

Judged from the kinetic plots of the mutants, V302D and L193E/V302D had almost lost the substrate inhibition.   As discussed in our previous studies of allosteric behaviour of *L. lactis* prolidase (Zhang et al., 2009), the interactions between the loop structure and Arg293 caused the allosteric behaviour by attracting the loop structure towards the active site.   When substrate concentration gets higher, the stabilization of loop structure by substrate binding increases to an extent that approach of substrate molecules is prevented, resulting in the substrate inhibition. Base on this speculation that the substrate inhibition is related to the allosteric behaviour, the loss of substrate inhibition in the mutant V302D and L193E/V302D could also be explained by the restriction imposed by Asp302 to the conformational change of the allosteric-determining site composed of the loop structure and Arg293, as discussed in the loss of allosteric behaviour.

In the model of V302D (Figure 5.3-1), an ionic bond was formed between Asp302 and Arg293 and the electrostatic attraction was exhibited between Asp302 and the zinc ion, causing the dissociation of residue Glu325 from the zinc ion near Asp302. Thus the allosteric-determining residue Arg293 was no longer associated with catalytic zinc ions via metal-chelating residue Glu325. This dissociation was also found in the model of the mutant L193E/V302D. Glu325 coordinated to both catalytic zinc ions, resulting in the dissociation with Arg293. However the dissociation was not observed in L193R/V302D. Then it was suggested that the dissociation of Arg293 with zinc ion was responsible to the loss of the substrate inhibition. In prolidases exhibiting substrate inhibition, the substrate binding might rearrange the interactions at residue Arg293 through the metal-chelating Glu325 residue and then restrict movements of Arg293 as substrate accumulated. Thus the above mentioned dissociation of Arg293 to metal-chelating residue or zinc ion resulted in the loss of substrate inhibition. This speculation was supported by the fact that R293S mutant also lost the substrate inhibition (Zhang et al., 2009). It was readily to say that the zinc-bound substrate molecule was no longer able to affect the position of Arg293 because of those dissociations of Arg293 from zinc ion in the V302D and L193R/V302D mutants.

In conclusions, Val302 was indicated as an important residue associated with both the allosteric behaviour and substrate inhibition in wild type prolidase. The loss of allosteric behaviour and substrate inhibition in L193R, L193T, V302D, L193R/V302D and L193E/V302D would be caused by restricting the movement of Arg293 via electrostatic attraction from Asp302 and the dissociation of Arg293 from catalytic zinc ions.

5.3.3.3 Allosteric mechanism

It was proposed that the allosteric behaviour and substrate inhibition had the same determining region in prolidase, which was defined by a loop structure (position 33 to 41 with charged residues Asp36, His38, Glu39 and Arg40 in the middle) and Arg293 as discussed in the previous sections (Zhang *et al.*, 2009). The allosteric behaviour was aroused by the conformational change between the tense (T) and relax (R) states. In the proposed model, the

loop structure was located closely to the active site on the other subunit of this homodimeric peptidase and associated with Arg293 near the active site. In this allostery model, prolidase adopts the T state with the loop structure residing closely to the active site and blocking the entering of substrate at lower substrate concentration. When substrate concentrations increase to a certain level, the binding of substrate molecules at the active site of one subunit induces that of the other subunit, causing the conformational change to the R state. At this state, the enzyme structure is more relaxed with the loop structure more open to the binding of more substrates. However, the substrate inhibition is presented when substrate concentrations are greater than a certain level. It is proposed in this project that the substrate inhibition follows the homotropic allostery (LiCata & Allewell, 1997). Two molecules of substrate accommodate at the active site to form an inactive ESS complex, and each subsite of active site in prolidase is occupied by a side chain from different molecule of substrates. This ESS complex differs from active ES complex based on the fact that only one molecule of substrate binds to the active site by its side chains bound to their corresponding subsites in the active form (Parkin, 2003).

Since prolidase is a homodimer and the allosteric region would be composed with the loop structure from subunit A and the active site pocket from subunit B, the mechanism of allosteric conformational changes is suggested as the second mechanism mentioned in the literature survey part (2.5.3 (ii)). The conformational change of one subunit would influence that of the other subunit. That is the binding of substrate molecule at the active site of subunit A would cause the conformational change of the loop structure in the same subunit, which constitutes an allosteric region with the active pocket of subunit B. The allosteric behaviour is then presented through the conformational change at the interface between two subunits, and determined by the different state of these subunits.

5.3.4 Thermal Dependency

Thermal dependency of each mutant was investigated by measuring activities of each enzyme at different temperatures. The observed activities were expressed as the relative activities to the activity of each prolidase towards Leu-Pro at 50 °C (Figure 5.3-4). All mutants

and wild type prolidase showed bell-shaped profiles of thermal dependency of activity (Figure 5.3-4). Most mutants exhibited a wider range of working temperature than the wild type did. To compare the differences of thermal dependences in details, the optimum temperatures of the wild type and mutants were calculated from the non-linear regression of curves of activity versus temperatures through statistical analyses (Table 5.3-6).

The results revealed that L193R, L193T, V302D, L193R/V302D and L193E/V302D had higher optimum temperatures (around 60 °C) than others (around 50 °C) (Table 5.3-6). It was interesting to notice that these mutants with higher optimum temperatures were observed to lose the allosteric behaviour. Many studies have suggested that suitable relaxation of the conformational rigidity was required for enzyme function (Hajdú et al., 2008; Hammes-Schiffer, 2002; Shoichet et al., 1995). If the mutated enzyme conformation has less flexibility compared to the wild type, a higher energy input would be required to achieve the flexibility of the mutated enzymes at the required levels for their enzyme activities. This higher energy input could be achieved by increasing the environmental temperature during the enzyme reaction, and the higher environmental temperature would give a faster enzyme reaction as far as the enzyme structure is not disturbed. Thus higher optimum temperatures would be observed; if the enzymes become more rigid.

It suggested that all the non-allosteric mutants possess more rigid conformations compared to the wild type. The rigidity was performed by the restriction of the conformational change observed at the allosteric region of non-allosteric mutants, which was composed with the loop structure and Arg293. In specific case of the V302D mutant, the restriction was presented by the opposite-charge attraction between the anionic substituted residue Asp302 and positively charged Arg293. As discussed, the loop structure and Arg293 would not interact in this mutant and it would restrict the structure variance in the allosteric behaviour. The loss of allostery means the enzymes do not have conformation changes between R and T states, thus, non-allosteric mutant prolidases would have more rigid conformation than the wild type. This indicated that the higher optimum temperatures of non-allosteric prolidases were the results of
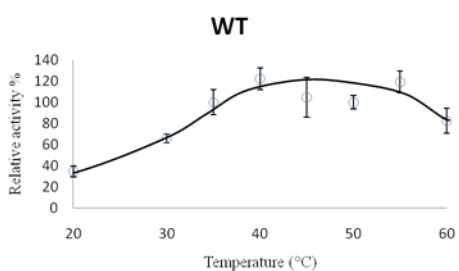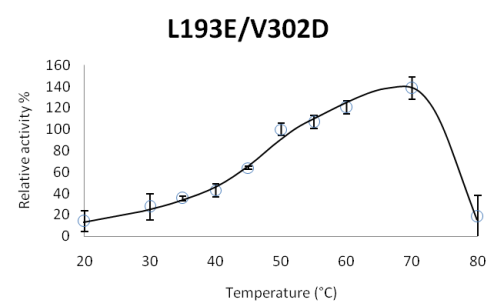
L193E

L193R

L193T

V302D

V302T

V302K

L193R/V302D

L193E/V302D

WT
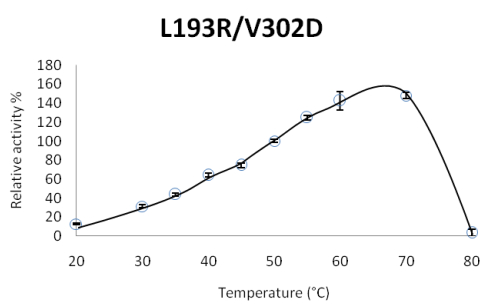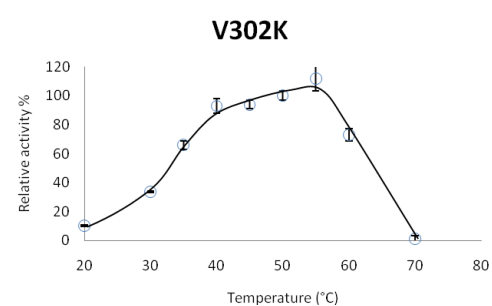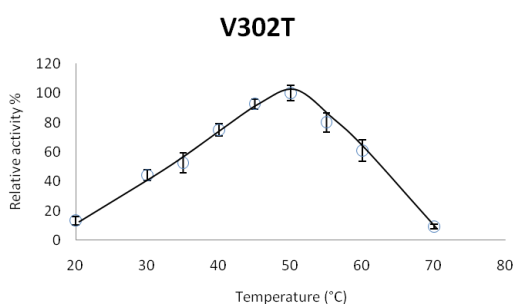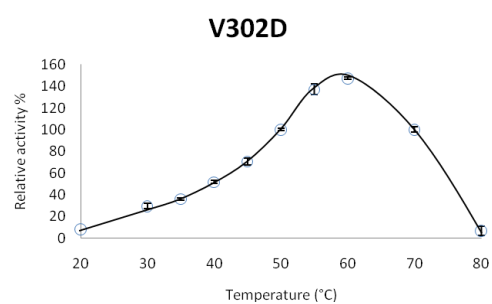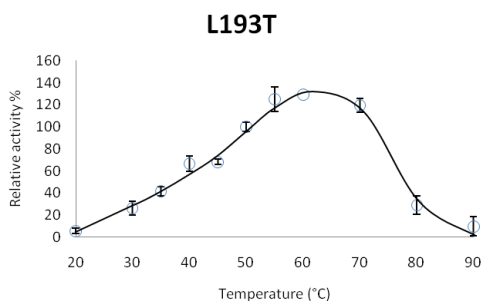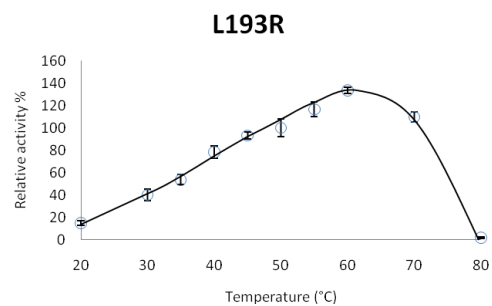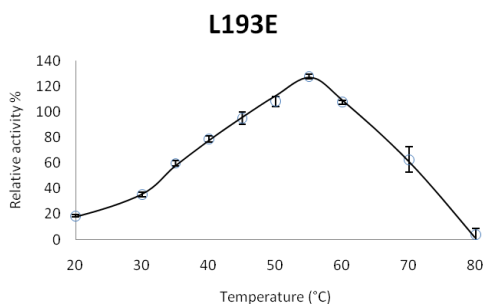
Figure 5.3-4 Thermal dependences of prolidases' activities.

The thermal dependency of each prolidase was presented as a plot of relative activities towards 2 mM Leu-Pro versus temperatures. The relative activities were calculated to the activity of each prolidase towards Leu-Pro at 50 °C.

Table 5.3-6 The optimum temperatures of enzymes

	Optimum Temperature (°C)	Residual standard error
WT	49.0	25.4
L193E	54.5	6.2
L193R	59.8	6.5
L193T	61.1	8.2
V302D	59.7	11.3
V302K	49.3	12.9
V302T	49.2	9.3
L193R/V302D	62.2	10.7
L193E/V302D	62.8	12.7

rigid structure due to the loss of allostery.

5.3.5 Metal Dependency

The metal dependency was investigated by measuring the activities of each mutant to eleven different dipeptide and tripeptide substrates after the substitution of Mn^{2+} for Zn^{2+} as the catalytic metal ions. Table 5.3-7 shows the relative activities of each mutant to eleven different substrates in the presence of Mn^{2+}, presented as the activity of each mutant relative to the activity on Leu-Pro.

It has been observed (Table 5.3-7) that the absolute activities were smaller in all mutants than in wild type prolidase, and were much larger in the presence of Mn^{2+} than Zn^{2+} in the anionic mutations L193E and V302D and in the hydrophilic L193T.

More detailed comparisons were deduced from Table 5.3-8 on the differences of mutants' activities with two catalytic ions. When comparing the preferences of the mutated prolidases, the L193E, L193R, L193T, V302D and V302T mutants showed much more preferences towards positively charged substrates Arg-Pro and Lys-Pro in the presence of Mn^{2+} than that with Zn^{2+}, while none of the Leu193 and Val302 mutants preferred negatively charged substrates Asp-Pro or Glu-Pro with Mn^{2+} presenting.

Manganese has many oxidation states (from –III to +VII), among which divalent manganese is the most stable oxidation state in acid and neutral solutions (Cotton, 1999). Divalent manganese has a ionic radius of 0.75 Å, which is close to the ionic radius of divalent zinc (0.74 Å) (Glusker, 1991). The predominant coordination number of Mn^{2+} is six, while four, five, six are common coordination numbers for Zn^{2+} based on the crystal structure analysis (Bock et al., 1999). In wild type prolidase, the higher activities to various substrates were generally shown in the presence of Zn^{2+} than that with Mn^{2+} in our previous study (Yang & Tanaka, 2008). The molecular modelling showed that five residues, Asp221, Asp232, His296, Glu325 and Glu339, are metal-chelating residues for the two catalytic zinc ions. By the consideration of the hydrophobic feature of the catalytic pocket in the wild type, the coordination number might be six for Mn^{2+} and four for Zn^{2+}, and there might be just one catalytic manganese ion in wild type

Table 5.3-7 The absolute activities of mutants to Leu-Pro with Zn^{2+}.

Metals	Specific activity(μmol/min·mg)								
	L193E	L193R	L193T	V302D	V302K	V302T	L193R/V302D	L193E/V302D	WT
Zn^{2+}	99.6±5.6	118.8±12.1	67.3±9.3	14.1±2.6	55.9±1.4	73.5±5.2	7.5±0.36	0.95±0.05	468.7
Mn^{2+}	234.3±8.3	54.4±2.5	406.4±7.76	97.1±3.2	47.0±4.4	88.8±10.3	5.6±0.08	0.8±0.14	234.5

Table 5.3-8 The substrate specificities of mutants in relative activities.

Substrates	Metals	Relative Activity (%)							
		L193E	L193R	L193T	V302D	V302K	V302T	L193R/V302D	L193E/V302D
Leu-Pro	Zn^{2+}	100.0	100.0	100.0	100.0	100.0	100.0	100.0	100.0
	Mn^{2+}	235.2	45.8	604.3	691.1	84.1	120.9	74.7	88.6
Phe-Pro	Zn^{2+}	33.3	20.2	278.6	59.3	8.8	14.5	21.9	180.0
	Mn^{2+}	114.7	24.5	886.6	186.7	35.1	71.9	7.9	51.1
Asp-Pro	Zn^{2+}	5.9	37	N.D.	25.9	2.6	3.4	33	16
	Mn^{2+}	5.7	7.9	2.8	57.8	0.0	2.1	50.6	27.3
Glu-Pro	Zn^{2+}	2	2.5	11.4	7.4	N.D.	2	24.9	20
	Mn^{2+}	8.4	16.3	20.8	5.5	0.0	3.8	29.4	27.5
Arg-Pro	Zn^{2+}	51	1.9	81.4	57.4	5.7	32.8	13.8	62
	Mn^{2+}	374.2	22.3	228.1	1381.1	19.4	69.6	30.1	56.7
Lys-Pro	Zn^{2+}	39.2	2.3	48.6	31.5	4.1	37.5	19.2	78

	Mn^{2+}	532.7	51.4	507.7	1797.8	1.2	85.2	21.6	29.7
	Zn^{2+}	70.6	11.1	34.3	N.D.	29.4	46	2.7	N.D.
Val-Pro	Mn^{2+}	212.1	94.9	265.4	564.4	31.1	88.5	5.6	20.8
	Zn^{2+}	N.D.	2.9	2.9	N.D.	N.D.	1	N.D.	N.D.
Gly-Pro	Mn^{2+}	13.3	3.2	14.3	75.5	0.1	9.6	1.7	0.0
	Zn^{2+}	3.9	0.7	14.3	7.4	N.D.	N.D.	N.D.	N.D.
Pro-Pro	Mn^{2+}	11.9	2.4	1.1	22.3	1.0	3.1	1.1	3.4
	Zn^{2+}	3.9	N.D.	N.D.	N.D.	N.D.	N.D.	N.D.	N.D.
Leu-Leu-Pro	Mn^{2+}	0.0	1.2	1.6	27.8	0.0	1.1	0.2	2.5
	Zn^{2+}	9.8	N.D.	N.D.	N.D.	N.D.	N.D.	N.D.	N.D.
Leu-Val-Pro	Mn^{2+}	3.7	0.5	0.8	26.1	0.1	0.0	0.0	2.0

prolidase instead of two zinc ions (Bock et al., 1999). The larger coordination number of Mn^{2+} meant less effective positive charge on the metal, leading to a higher pK_a of Mn^{2+}-bound water. In other words, the Mn^{2+} had weaker metal-ligand bindings due to its larger coordination number, resulting in a weaker polarization of O-H in the intermediate anion of Mn^{2+}-OH, and thus the Mn^{2+}-bound water has a higher pK_a. Then the higher pK_a of Mn^{2+}-bound water caused a reduced electron deficiency of the metal ion centre, which stabilized less negative charge developed on the substrate peptide carbonyl oxyanion during the nucleophilic attack. It was proposed that the changes of the charge states on the S_1 site residues and the choice of the polarity of side chains of the P_1 residue affected the relative coordination of the chelating residues to metal cations and that they led to the changes in the activity through pK_a modifications. This proposal needs to be investigated in the future research, such as X-ray crystallography.

The possible higher pK_a of Mn^{2+}-bound water than Zn^{2+}-bound water might explain the large increases in absolute activities observed in L193E, L193T, V302D and V302T mutants in the presence of Mn^{2+}. In previous discussion, His296 was proposed to be the proton acceptor receiving protons from water molecules in the catalysis of prolidase. The introduced charge by mutated residues could influence its electronic state, thus to affect the catalytic efficiency. It was possible that the catalytic Mn^{2+} together with His296 performed different extent of influence on the mutants. The introduction of negatively charged residues glutamate and aspartate in the L193E and V302D mutants would stabilize His296 in protonated form through the opposite-charge attraction. The protonation of His296 was negative for its performance as a proton acceptor, resulting in depressed catalytic efficiency. The less depression in the presence of Mn^{2+} (the absolute activities of L193E and V302D were lower than wild type, but higher with Mn^{2+} than with Zn^{2+}) was suggested to relate to the higher pK_a of Mn^{2+}-bound water than Zn^{2+}-bound water.

In the comparisons of mutants' substrate specificities, the preferences of positively charged substrates to negatively charged substrates were observed in most mutants as stated before. This

observation might also be explained by the higher pK_a of Mn^{2+}-bound water than Zn^{2+}-bound water. Further research is needed for understanding the influence of catalytic metals on substrate specificities of prolidases.

For a conclusion, catalytic metals with different pK_a values were suggested to work with the proton acceptor His296 to influence the catalytic efficiencies of different mutated prolidases. The different profiles of substrate specificities of mutants with different catalytic metals might relate to the different pK_a values of metal-bound water during the nucleophilic attack. More detailed research, *e.g.* X-ray crystallography, is needed to further elucidate the structural differences of mutated prolidases in the presence of different metals.

6 GENERAL CONCLUSIONS

A series of studies have been designed and implemented on the mutated prolidases' characteristics, including substrate specificity, pH dependency, allosteric behaviour, thermal dependency and metal dependency, to investigate the roles of three residues Phe190, Leu193 and Val302 in the structure-function relationship of prolidases. The experimental results were analyzed together with the molecular modelling to be shown as following.

Substrate specificity towards hydrophobic Xaa-Pro dipeptides was determined by Leu193 and Val302. Especially Leu193 showed more influence on prolidase's substrate specificity shown by the several facts: the substitutions of Leu193 by charged residues improved the prolidase's preferences towards the dipeptide substrates which had opposite charge to the mutated residue; the V302D mutant took both anionic Asp-Pro and cationic Arg-Pro as substrates, due to its interactions with neighbouring cationic residues Arg293 and His296 which generated a hydrophilic substrate binding site. The close location of Val302 to Arg293 was then suggested to cause the loss of allosteric behaviour in the kinetic studies of prolidase. This finding proves that Arg293 is a key residue in the allosteric behaviour by constituting the allosteric region with the loop structure. The catalytic efficiency was influenced by both Leu193 and Val302 mutations, with Val302 having more effect on it. This was because the location of Val302 was nearer to His296 than that of Leu193, and His296 was proposed to be involved in the catalytic centre as the proton acceptor. Because His296 would lose its capability of being a proton acceptor when it became protonated at pHs lower than 6.0, wild type prolidase lost the activity at these pHs. However, the mutated prolidases were observed to have extended working pH ranges towards the acidic conditions compared to the wild type, indicating that the catalytic role of His296 was retained at lower pHs in these mutants through interactions with charged substituted residues at the S_1 site. Furthermore, the changes of pH ranges were observed in the

comparisons within each mutant prolidase in the presence of different charged substrates. It was suggested that the positively charged substrate would also influence the electrostatic form of His296 and thus would affect the catalysis of prolidases.

7 FUTURE RESEARCH

Currently the functions of the loop structure are being investigated by Dr. Tanaka's research group to elucidate more details of the catalytic mechanisms and to modify *L. lactis* prolidase for the debittering applications. The mutations on the loop, including substitution, deletion or addition, would be considered to examine the interactions of the loop to other residues in the prolidase structure. It will clarify how this loop structure is involved in the allosteric behaviour, substrate inhibition, and other kinetic characteristics. Also the role of His296 as the proton acceptor in the catalysis of prolidase will be elucidated via more direct experiments focusing on it. These results will be combined to develop mutant prolidases that are efficient to remove the bitterness.

8 REFERENCES

Arata, J., Umemura, S. & Yamamoto, Y. (1979) Prolidase deficiency. Its dermatological manifestations and some additional biochemical studies. *Arch Dermatol* **115**, 62-67.

Badarau, A. & Page, M. I. (2006) The Variation of Catalytic Efficiency of *Bacillus cereus* Metallo-*β*-lactamase with Different Active Site Metal Ions. *Biochemistry* **45**, 10654-10666.

Barrett, A. J. (2001) Proteolytic enzymes: nomenclature and classification. In *Proteolytic enzymes*. Edited by R. Beynon & J. S. Bond. New York: Oxford university press.

Bock, C. W., Katz, A. K., Markham, G. D. & Glusker, J. P. (1999) Manganese as a Replacement for Magnesium and Zinc: Functional Comparison of the Divalent Ions. *J Am Chem Soc* **121**, 7360-7372.

Brosset, B., Myara, I., Fabre, M. & Lemonnier, A. (1988) Plasma prolidase and prolinase activity in alcoholic liver disease. *Clin Chim Acta* **175**, 291-295.

Brown, T. A. (2001) *Essential molecular biology: a practical approach*, 2nd edn. New York: Oxford University Press.

Buffa, M., Guamis, B. & Trujillo, A. J. (2005) Specific effect of high-pressure treatment of milk on cheese proteolysis. *J Dairy Res* **72**, 385-392.

Casey MG, M. J. (1985) Presence of X-prolyl-dipeptidyl-peptidase in lactic acid bacteria. *J Dairy*

Sci **68**, 3212-3215.

Chien, C. H., Huang, L. H., Chou, C. Y., Chen, Y. S., Han, Y. S., Chang, G. G., Liang, P. H. & Chen, X. (2004) One site mutation disrupts dimer formation in human DPP-IV proteins. *J Biol Chem* **279**, 52338-52345.

Christensen, J. E., Dudley, E. G., Pederson, J. A. & Steele, J. L. (1999) Peptidases and amino acid catabolism in lactic acid bacteria. *Antonie van Leeuwenhoek* **76**, 217-246.

Cole, R. & Loria, J. P. (2002) Evidence for flexibility in the function of ribonuclease A. *Biochemistry* **41**, 6072-6081.

Cosson, C., Myara, I., Miech, G., Moatti, N. & Lemonnier, A. (1992) Only prolidase I activity is present in human plasma. *Int J Biochem* **24**, 427-432.

Cotton, F. A. (1999) *Advanced inorganic chemistry*, 6th edn. New York: John Wiley and Sons.

Crawley, M. J. (2007) *The R Book*. West Sussex: John Wiley & Sons Ltd.

Cunningham, D. F. (1997) Proline specific peptidases. *Biochim Biophys Acta* **1343**, 160-186.

Davis, N. C. & Smith, E. L. (1957) Purification and some properties of prolidase of swine kidney. *J Biol Chem* **224**, 261-275.

de Kreij, A., van den Burg, B., Veltman, O. R., Vriend, G., Venema, G. & Eijsink, V. G. H. (2001) The effect of changing the hydrophobic S_1 subsite of thermolysin-like proteases on substrate specificity. *Eur J Biochem* **268**, 4985-4991.

Doi, E., Shibata, D. & Matoba, T. (1981) Modified colorimetric ninhydrin methods for peptidase assay. *Anal Biochem* **118**, 173-184.

Endo, F., Hata, A., Indo, Y., Motohara, K. & Matsuda, I. (1987) Immunochemical analysis of prolidase deficiency and molecular cloning of *c*DNA for prolidase of human liver. *J Inherit Metab Dis* **10**, 305-307.

Eriksson, A. E., Baase, W. A., Wozniak, J. A. & Matthews, B. W. (1992) A cavity-containing mutant of T4 lysozyme is stabilized by buried benzene. *Nature* **355**, 371-373.

Falzone, C. J., Wright, P. E. & Benkovic, S. J. (1994) Dynamics of a flexible loop in dihydrofolate reductase from *Escherichia coli* and its implication for catalysis. *Biochemistry* **33**, 439-442.

Fernandez-Espla, M. D., Martin-Hernandez, M. C. & Fox, P. F. (1997) Purification and characterization of a prolidase from *Lactobacillus casei* subsp *casei* IFPL 731. *Appl Environ Microbiol* **63**, 314-316.

Gejyo, F., Kishore, B. K. & Arakawa, M. (1983) Prolidase and prolinase activities in the erythrocytes of patients with chronic uremia. *Nephron* **35**, 58-61.

Gerhartz, B., Niestroj, A. J. & Demuth, H.-U. (2002) Enzyme classes and mechanisms. In *Proteinase and peptidase inhibition*. Edited by H. J. Smith & C. Simons. New York: Taylor & Francis Inc.

Ghadimi, H. & Pecora, P. (1963) Free amino acids of different kinds of milk. *Am J Clin Nutr* **13**,

75-81.

Glusker, J. P. (1991) Structural aspects of metal liganding to functional groups in proteins. *Advances in Protein Chemistry* **42**, 1-76.

Goodman, S. I., Solomons, C. C., Muschenheim, F., McIntyre, C. A., Miles, B. & O'Brien, D. (1968) A syndrome resembling lathyrism associated with iminodipeptiduria. *Am J Med* **45**, 152-159.

Gross, R. L. (2000) The effect of ascorbate on wound healing. *Int Ophthalmol Clin* **40**, 51-57.

Guedon, E., Renault, P., Ehrlich, S. D. & Delorme, C. (2001) Transcriptional pattern of genes coding for the proteolytic system of *lactococcus lactis* and evidence for coordinated regulation of key enzymes by peptide supply. *J Bacteriol* **183**, 3614-3622.

Hajdú, I., Bőthe, C., Szilágyi, A., Kardos, J., Gál, P. & Závodszky, P. (2008) Adjustment of conformational flexibility of glyceraldehyde-3-phosphate dehydrogenase as a means of thermal adaptation and allosteric regulation. *Eur Biophy J* **37**, 1139-1144.

Hammes-Schiffer, S. (2002) Impact of enzyme motion on activity. *Biochemistry* **41**, 13335-13343.

Harris, T. K. & Turner, G. J. (2002) Structural basis of perturbed pK_a values of catalytic groups in enzyme active sites. *IUBMB Life* **53**, 85.

Hartley, B. S. (1960) Proteolytic enzymes. *Annu Rev Biochem* **29**, 45-72.

Heyde, E. (1976) A unifying concept for the active site region in aspartate transcarbamylase. *Biochim Biophys Acta - Enzymology* **452**, 81-88.

Humphrey, W., Dalke, A. & Schulten, K. (1996) VMD: Visual molecular dynamics. *J Mol Graph* **14**, 33-38.

Ishibashi, N., Kouge, K., Shinoda, I., Kanehisa, H. & Okai, H. (1988a) A mechanism for bitter taste sensibility in peptides. *Agric Biol Chem* **52**, 819-827.

Ishibashi, N., Kubo, T., Chino, M., Fukui, H., Shinoda, I., Kikuchi, E., Okai, H. & Fukui, S. (1988b) Taste of proline-containing peptides. *Agric Biol Chem* **52**, 95-98.

Jaenicke, R. & Závodszky, P. (1990) Proteins under extreme physical conditions. *FEBS Lett* **268**, 344-349.

Kadonosono, T., Kato-Murai, M. & Ueda, M. (2008) Alteration of substrate specificity of rat neurolysin from matrix metalloproteinase-2/9-type to-3-type specificity by comprehensive mutation. *Protein Eng Des Sel* **21**, 507-513.

Kal, L., Skeel, R., Bhandarkar, M. & other authors (1999) NAMD2: Greater scalability for parallel molecular dynamics. *J Comput Phys* **151**, 283-312.

Kaplan, W. & Littlejohn, T. G. (2001) Swiss-PDB Viewer (deep view). *Brief Bioinform* **2**, 195-197.

Kobasa, D., Kodihalli, S., Luo, M., Castrucci, M. R., Donatelli, I., Suzuki, Y., Suzuki, T. & Kawaoka, Y. (1999) Amino acid residues contributing to the substrate specificity of the influenza

A virus neuraminidase. *J Virol* **73**, 6743-6751.

Kunji, E. R. S., Mierau, I., Hagting, A., Poolman, B. & Konings, W. N. (1996) The proteolytic systems of lactic acid bacteria. *Antonie Van Leeuwenhoek* **70**, 187-221.

Kusano, M., Yasukawa, K., Hashida, Y. & Inouye, K. (2006) Engineering of the pH-dependence of thermolysin activity as examined by site-directed mutagenesis of Asn112 located at the active site of thermolysin. *J Biochem* **139**, 1017-1023.

Lee, S., Oneda, H., Minoda, M., Tanaka, A. & Inouye, K. (2006) Comparison of starch hydrolysis activity and thermal stability of two *Bacillus licheniformis* α-amylases and insights into engineering α-amylase variants active under acidic conditions. *J Biochem* **139**, 997-1005.

LiCata, V. J. & Allewell, N. M. (1997) Is substrate inhibition a consequence of allostery in aspartate transcarbamylase? *Biophys Chem* **64**, 225-234.

Lin, X. L., Wong, R. N. & Tang, J. (1989) Synthesis, purification, and active site mutagenesis of recombinant porcine pepsinogen. *J Biol Chem* **264**, 4482-4489.

Lin, Y., Fusek, M., Lin, X., Hartsuck, J. A., Kezdy, F. J. & Tang, J. (1992) pH dependence of kinetic parameters of pepsin, rhizopuspepsin, and their active-site hydrogen bond mutants. *J Biol Chem* **267**, 18413-18418.

Lipscomb, W. N. & Strater, N. (1996) Recent advances in zinc enzymology. *Chem Rev* **96**, 2375-2434.

Matthews, B. W. (1988) Structural basis of the action of thermolysin and related zinc peptidases.

Acc Chem Res **21**, 333-340.

Mock, W. L. & Aksamawati, M. (1994) Binding to thermolysin of phenolate-containing inhibitors necessitates a revised mechanism of catalysis. *Biochem J* **302**, 57-68.

Morel, F., Frot-Coutaz, J., Aubel, D., Portalier, R. & Atlan, D. (1999) Characterization of a prolidase from *Lactobacillus delbrueckii* subsp. *bulgaricus* CNRZ 397 with an unusual regulation of biosynthesis. *Microbiology* **145**, 437-446.

Myara, I., Cosson, C., Moatti, N. & Lemonnier, A. (1994) Human kidney prolidase-purification, preincubation properties and immunological reactivity. *Int J Biochem* **26**, 207-214.

Ohhashi, T., Ohno, T., Arata, J., Sugahara, K. & Kodama, H. (1990) Characterization of prolidase I and II from erythrocytes of a control, a patient with prolidase deficiency and her mother. *Clin Chim Acta* **187**, 1-9.

Palmer, D. R. J., Garrett, J. B., Sharma, V., Meganathan, R., Babbitt, P. C. & Gerlt, J. A. (1999) Unexpected Divergence of enzyme function and sequence: "n-acylamino acid racemase" is o-succinylbenzoate synthase. *Biochemistry* **38**, 4252-4258.

Parkin, K. L. (2003) Putting kinetic principles into practice. In *Enzyme kinetics: a modern approach*. Edited by A. G. Marangoni. Hoboken: John Wiley & Sons.

Pelmenschikov, V., Blomberg, M. & Siegbahn, P. (2002) A theoretical study of the mechanism for peptide hydrolysis by thermolysin. *J Biol Inorg Chem* **7**, 284-298.

Petranovic, D., Guedon, E., Sperandio, B., Delorme, C., Ehrlich, D. & Renault, P. (2004)

Intracellular effectors regulating the activity of the *Lactococcus lactis* CodY pleiotropic transcription regulator. *Mol Microbiol* **53**, 613-621.

Price, N. C. (1999) *Fundamentals of enzymology: the cell and molecular biology of catalytic proteins*, 3rd edn. Oxford: Oxford University Press.

Rantanen, T. & Palva, A. (1997) *Lactobacilli* carry cryptic genes encoding peptidase-related proteins: characterization of a prolidase gene (*pep*Q) and a related cryptic gene (*orf*Z) from *Lactobacillus delbrueckii* subsp. *bulgaricus*. *Microbiology* **143**, 3899-3905.

Scrutton, N. S., Deonarain, M. P., Berry, A. & Perham, R. N. (1992) Cooperativity induced by a single mutation at the subunit interface of a dimeric enzyme: glutathione reductase. *Science* **258**, 1140-1143.

Shenoy, A. R. & Visweswariah, S. S. (2003) Site-directed mutagenesis using a single mutagenic oligonucleotide and *Dpn*I digestion of template DNA. *Anal Biochem* **319**, 335-336.

Shoichet, B. K., Baase, W. A., Kuroki, R. & Matthews, B. W. (1995) A relationship between protein stability and protein function. *Proc Natl Acad Sci U S A* **92**, 452-456.

Sjostrom, H., Noren, O. & Josefsson, L. (1973) Purification and specificity of pig intestinal prolidase. *Biochim Biophys Acta* **327**, 457-470.

Stucky, K., Klein, J. R., Schueller, A., Matern, H., Henrich, B. & Plapp, R. (1995) Cloning and DNA sequence analysis of *pep*Q, a prolidase gene from *Lactobacillus delbrueckii* subsp. *lactis* DSM7290 and partial characterization of its product. *Mol Gen Genet* **247**, 494-500.

Tatsumi, C., Hashida, Y., Yasukawa, K. & Inouye, K. (2007) Effects of site-directed mutagenesis of the surface residues Gln128 and Gln225 of thermolysin on its catalytic activity. *J Biochem* **141**, 835-842.

Thomas, P. G., Russell, A. J. & Fersht, A. R. (1985) Tailoring the pH dependence of enzyme catalysis using protein engineering. *Nature* **318**, 375-376.

Traut, T. (2008a) Kinetics of allosteric enzymes. In *Allosteric Regulatory Enzymes*, pp. 77-102.

Traut, T. (2008b) Introduction to enzymes. In *Allosteric Regulatory Enzymes*, pp. 3-28.

Uramatsu, M., Liu, G., Uramatsu, S., Zhang, M., Wang, W., Nakayama, K., Manabe, M. & Kodama, H. (2007) Different effects of sulfur amino acids on prolidase and prolinase activity in normal and prolidase-deficient human erythrocytes. *Clin Chim Acta* **375**, 129-135.

Van den Burg, B., Dijkstra, B. W., Vriend, G., Van der Vinne, B., Venema, G. & Eijsink, V. G. (1994) Protein stabilization by hydrophobic interactions at the surface. *Eur J Biochem / FEBS* **220**, 981-985.

Verzani, J. (2005) *Using R For Introductory Statistics*. Boca Raton: Chapman & Hall.

Wang W, M. B. (1999) Two-stage PCR protocol allowing introduction of multiple mutations, deletions and insertions using QuikChange Site-Directed Mutagenesis. *Biotechniques* **26**, 680-682.

Whitehurst, C. B., Willis, J. H., Sinodis, C. N., Hernandez, R. & Brown, D. T. (2006) Single and multiple deletions in the transmembrane domain of the Sindbis virus E2 glycoprotein identify a

region critical for normal virus growth. *Virology* **347**, 199-207.

Xin, W., Huang, D.-W., Zhang, Y.-M. & Geng, L. (2004) DNA mutagenesis using T4 DNA polymerase and *Dpn*I restriction endonuclease. *Anal Biochem* **329**, 151-153.

Yang, S. I. & Tanaka, T. (2008) Characterization of recombinant prolidase from *Lactococcus lactis* changes in substrate specificity by metal cations, and allosteric behavior of the peptidase. *FEBS J* **275**, 271-280.

Yevenes, A., Espinoza, R., Rivas-Pardo, J. A., Villarreal, J. M., Gonzalez-Nilo, F. D. & Cardemil, E. (2006) Site-directed mutagenesis study of the microenvironment characteristics of Lys213 of *Saccharomyces cerevisiae* phosphoenolpyruvate carboxykinase. *Biochimie* **88**, 663-672.

Yoshida, Y., Ohkuri, T., Kino, S., Ueda, T. & Imoto, T. (2005) Elucidation of the relationship between enzyme activity and internal motion using a lysozyme stabilized by cavity-filling mutations. *Cell Mol Life Sci (CMLS)* **62**, 1047-1055.

Yoshimoto, T., Matsubara, F., Kawano, E. & Tsuru, D. (1983) Prolidase from bovine intestine: Purification and characterization. *J Biochem* **94**, 1889-1896.

Zhang, G., Chen, J. A. & Tanaka, T. (2009) Deregulation of allosteric response of *Lactococcus lactis* prolidase and its effects on enzyme activity. *Biochem Biophys Acta Protein Proteomics* **1794**, 968-975.

Zomer, A. L., Buist, G., Larsen, R., Kok, J. & Kuipers, O. P. (2007) Time-resolved determination of the CcpA regulon of *Lactococcus lactis* subsp. *cremoris* MG1363. *J Bacteriol* **189**, 1366-1381.

APPENDIX A

JUSTIFICATIONS OF STATISTICAL MODELS

Applicability of ANOVA Model in the Study of Substrate Specificity

The plots checking the ANOVA model were shown in Figure A-1. The first plot (top left) showed no pattern of the scattering points, approving the most important assumption of constancy of variance. According to the assumption of normal distribution of errors, the normal QQ plot (top right) should be a straight-line between standardized residuals and theoretical quantiles. However this plot appeared in a long-symmetric shape, which deviated from the straight line at two ends (Verzani, 2005). The residuals were well distributed in the Scale-location plot (bottom left). The Constant-leverage plot (bottom right) also showed the evenly distributed residuals versus factor levels. In a conclusion, the assumptions of ANOVA model were generally satisfied. So the results obtained from the nested ANOVA model could be employed for interpretations of the substrate specificity.

Applicability of Statistical Models in the Study of pH Dependency

To check the assumption of the GAM model, the significances (p-values) of several parameters were analyzed, such as smooth terms, values of R-squares and explained deviances from the GAM models of the research objects (Table A-1). All the smooth terms were significant with p-values smaller than 0.001 (merited three asterisks), and the values of R-squared and explained deviance were close to 1, indicating good model-fittings.

The applicability of the ANOVA model was checked by plotting (Figure A-2). The first plot displayed a scattering pattern of several perpendicular lines, and the points of residual versus fitted were evenly distributed on both sides of the horizontal line. This distribution was acceptable for the assumption of constancy of variance. In the normal QQ plot, the residuals
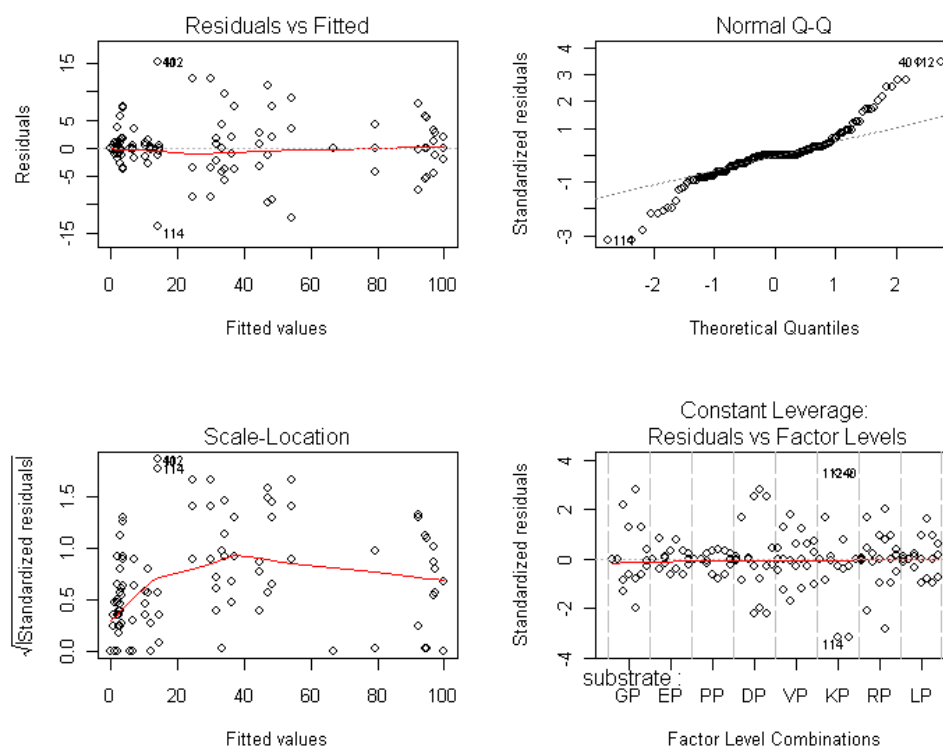
Figure A-1 The plots to check the ANOVA model assumption in the study of substrate specificity.

Table A-1 Summaries of GAM models in the study of pH dependency.

	p-value								
	LE.LP	LE.RP	LR.DP	LR.LP	VD.DP	VD.LP	VD.RP	WT.LP	WT.RP
s (pH)	<2e-16***	<2e-16***	3.73e-06***	<2e-16***	2.81e-16***	<2e-16***	<2e-16***	6.7e-10***	<2e-16***
R^2	0.987	0.985	0.714	0.99	0.965	0.989	0.973	0.904	0.988
Deviance explained	99.10%	98.90%	78.20%	99.30%	97.50%	99.20%	98.10%	93.20%	99.10%

Significant codes: *** $P <0.001$, ** $P <0.01$, *$P < 0.1$.
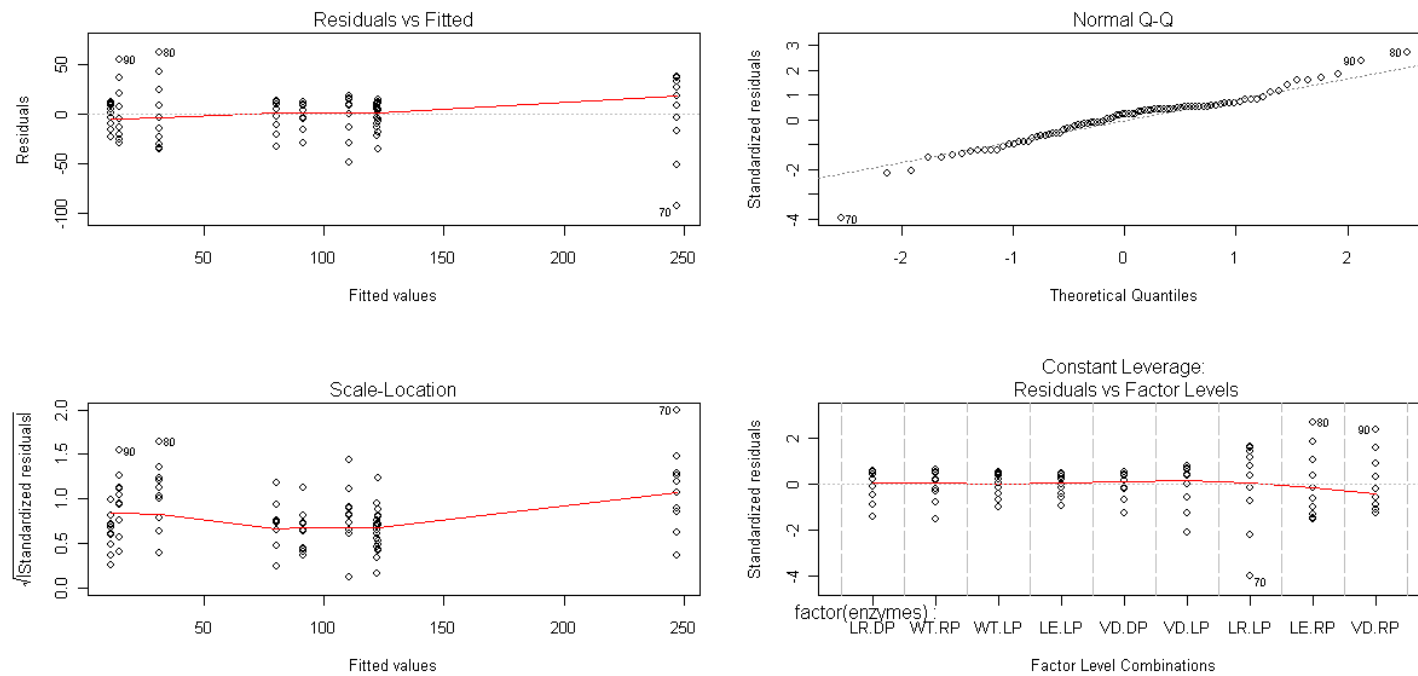
Figure A-2 The plots to check the ANOVA model assumptions in the study of pH dependency

and theoretical quantiles generally formed a straight line, which was the sign of the normal distribution of errors. The scale-location and leverage plots both exhibited evenly distributed residuals. In a conclusion, the ANOVA model appropriately fitted the slope data and its results were useful to interpret the results from the study of pH dependency.

APPENDIX B

STATISTICAL ANALYSES

The Bwplots of Relative Activities to Different Substrates

The relative activities to different substrates were plotted statistically for each enzyme in bwplots using ANOVA model, having the activity to substrate Leu-Pro as 100% (Figure B-1). The relative activities of mutant were compared with that of WT to a certain substrate. The numerous differences were calculated from these plots by taking a difference between mean activity of a mutant to a substrate and that of WT to the same substrate. The results are concluded in Table 5.3-2.

The Coplots of Relative Activities vs. pHs for Prolidases

The coplots were calculated using the GAM model in the R software, showing the statistical regression on prolidases' activities versus pH values in the presence of substrate Leu-Pro (Figure B-2) or Arg-Pro, Leu-Pro and Asp-Pro (Figure B-3). These statistically generated regression curves of activities versus pHs (Figure B-2 and B-3) were in accordance to the estimated bell-shaped curves (Figure 5.3-3). The slopes of the regression curves for each 0.5 increment (Table 5.3-3) were calculated out of these coplots, and were used to compare the effects of pH changes among enzymes and substrates.

The Slopes of the Regression Curves of Enzymes' pH Dependency

Each little box in the boxplot (Figure B-4) represented the slopes of activity changes between pH 5.0 and pH 5.5 in a mutated prolidase, with the middle line referring to the average value. The differences of the activity changes between prolidases were then calculated using the mean values of the slopes. And some results are presented and discussed in section 5.3.2.
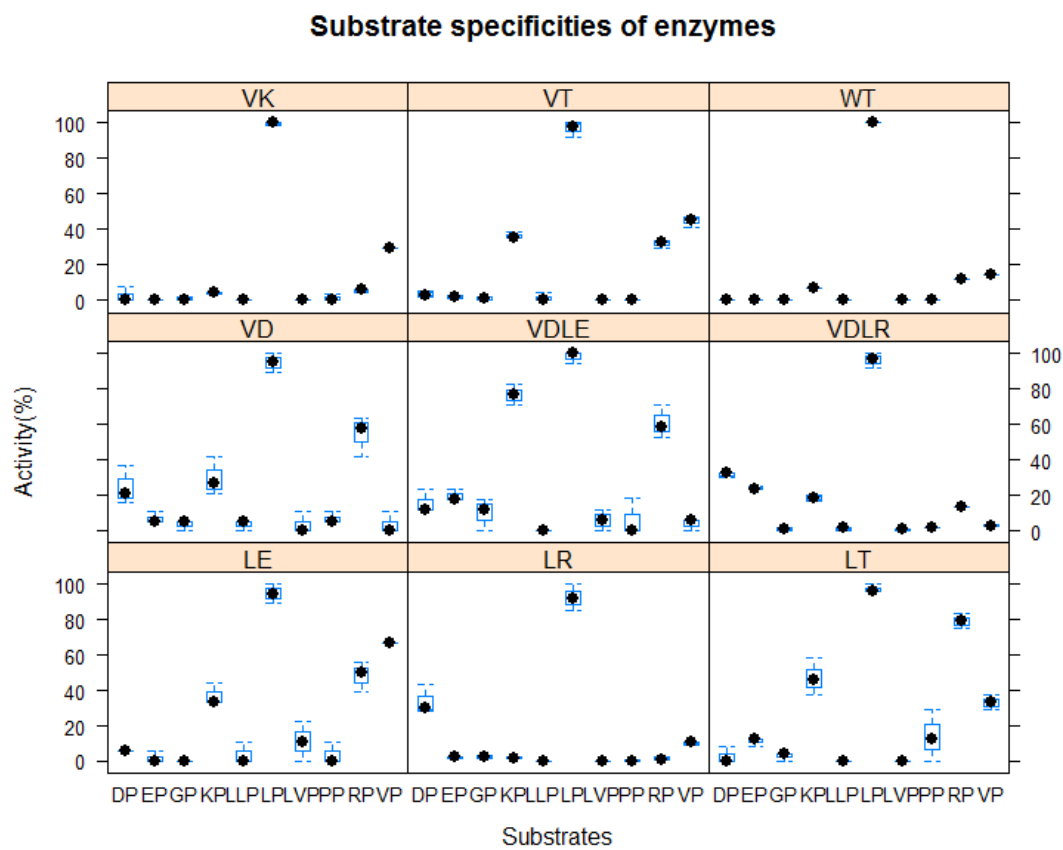
Figure B-1 The bwplots of activities versus substrates in different enzymes.

Enzymes are shortened as: "LE", L193E; "LR", L193R; "LT", L193T; "VD", V302D; "VDLE", L193E/V302D; "VDLR", L193R/V302D; "VK", V302K; "VT", V302T; "WT", wild type prolidase. Substrates are shorten as: "DP", Asp-Pro; "EP", Glu-Pro; "GP", Gly-Pro; "KP", Lys-Pro; "LP", Leu-Pro; "PP", Pro-Pro; "RP", Arg-Pro; "VP", Val-Pro.
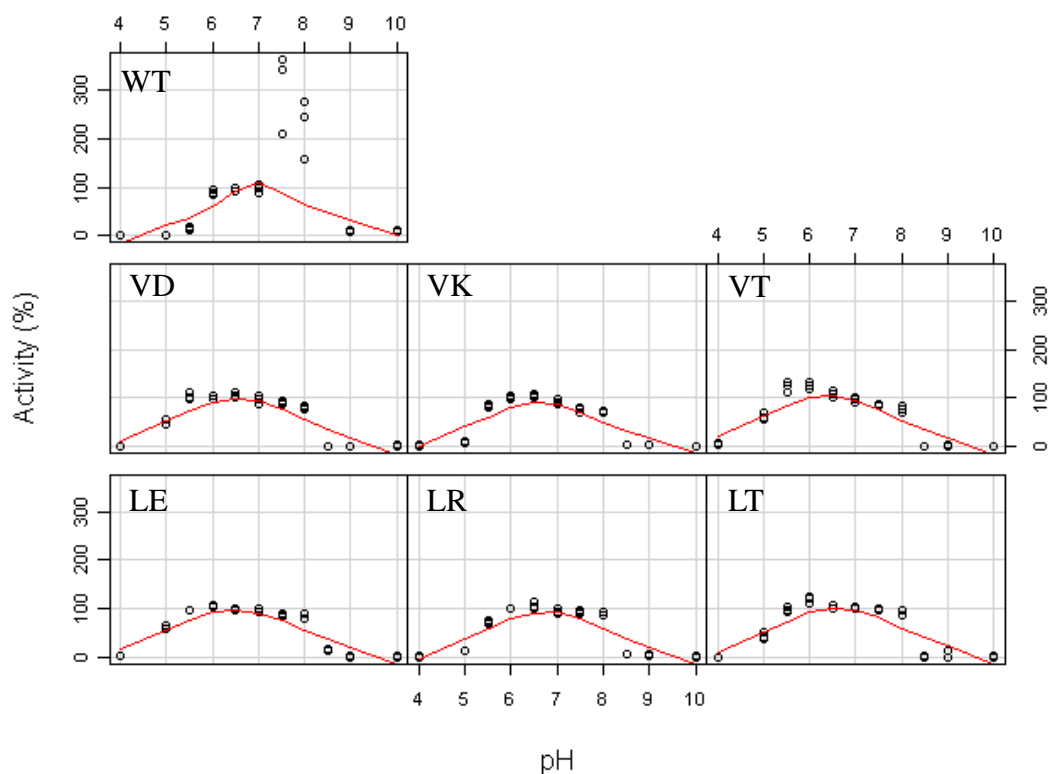
Figure B-2 The coplot of non-linear regression curves of prolidases with substrate Leu-Pro.

Each panel of the coplot depicts the activities of a prolidase at different pHs using 2 mM Leu-Pro as the substrate.

Symbols interpretations: "LE", L193E; "LR", L193R; "LT", L193T; "VD", V302D; "VK", V302K; "VT", V302T; "WT", wild type prolidase.
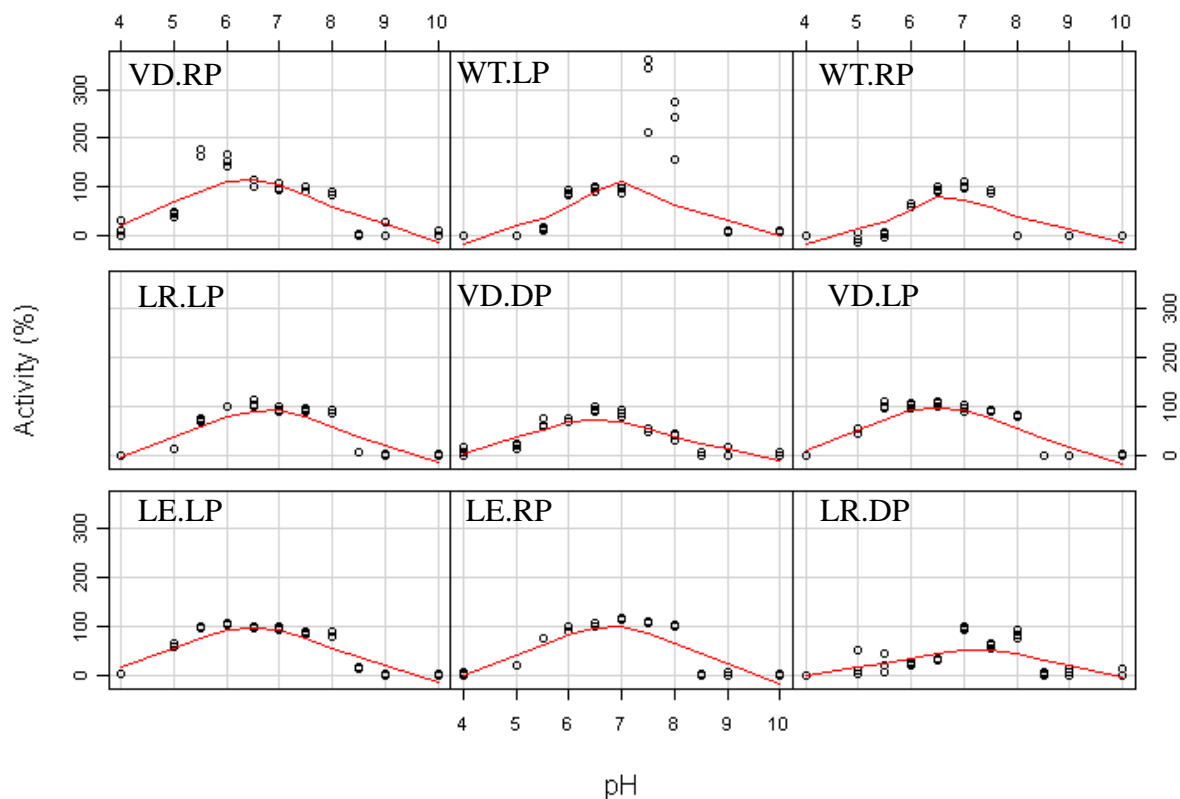
97

Figure B-3 The coplot of non-linear regression curves of prolidases with different substrates.

Each panel of the coplot depicts the activities of a prolidase at different pHs using 2 mM Leu-Pro, Arg-Pro or Asp-Pro as the substrate.

Symbols interpretations: "LE.LP", L193E to substrate Leu-Pro; "LE.RP", L193E to substrate Arg-Pro; "LR.DP", L193R to substrate Asp-Pro; "LR.LP", L193R to substrate Leu-Pro; "VD.DP", V302D to substrate Asp-Pro; "VD.LP", V302D to substrate Leu-Pro; "VD.RP", V302D to substrate Arg-Pro; "WT.LP", wild type prolidase to substrate Leu-Pro; "WT.RP", wild type prolidase to substrate Arg-Pro.

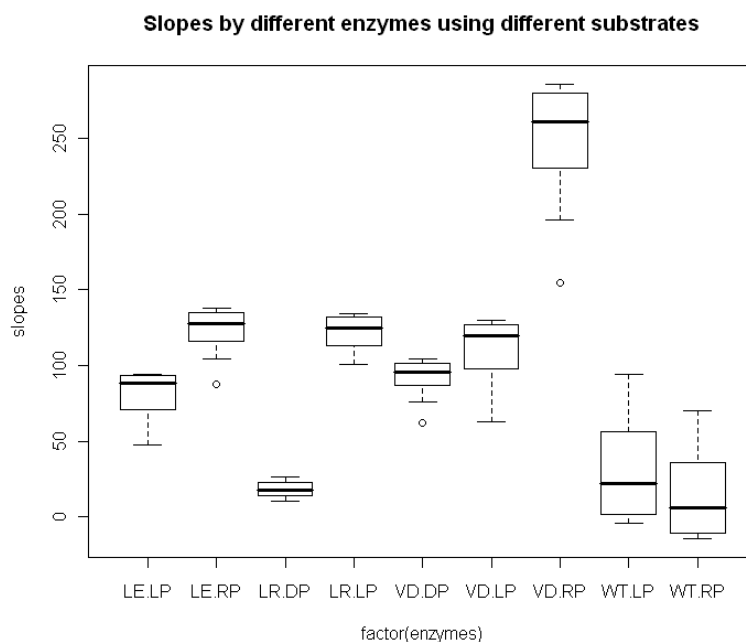**Slopes by different enzymes using different substrates**

Figure B-4 The boxplot of ANOVA analysis on slopes of the non-linear regression curves of enzymes' pH dependency in the range of pH 5.0~5.5.

Symbols interpretations: "LE.LP", L193E to substrate Leu-Pro; "LE.RP", L193E to substrate Arg-Pro; "LR.DP", L193R to substrate Asp-Pro; "LR.LP", L193R to substrate Leu-Pro; "VD.DP", V302D to substrate Asp-Pro; "VD.LP", V302D to substrate Leu-Pro; "VD.RP", V302D to substrate Arg-Pro; "WT.LP", wild type prolidase to substrate Leu-Pro; "WT.RP", wild type prolidase to substrate Arg-Pro.

VITA

Keke Hu was born in Beijing, China. After completing her study at Wuchang Experimental High School in Wuhan, China, she entered East China University of Science and Technology (ECUST) in Shanghai, China. She received her degree of Bachelor of Engineering in Biology Engineering from ECUST in July 2004. After graduation, she worked as a laboratory assistant for two years in the Bio- and Environmental Geology Laboratory in China University of Geosciences, Wuhan, China. In September 2006, she enrolled the graduate program of Applied Microbiology in the Department of Food and Bioproduct Sciences, College of Agriculture and Bioresources at University of Saskatchewan. On the basis of her Master Thesis she has published a paper "S_1 site residues of *Lactococcus lactis* prolidase affect substrate specificity and allosteric behaviour" in *Biochimica et Biophysica Acta (BBA) - Proteins & Proteomics* (Volume 1794, Issue 12, December 2009, Pages 1715-1724).

Contact the author via email: corrine_hu@hotmail.com